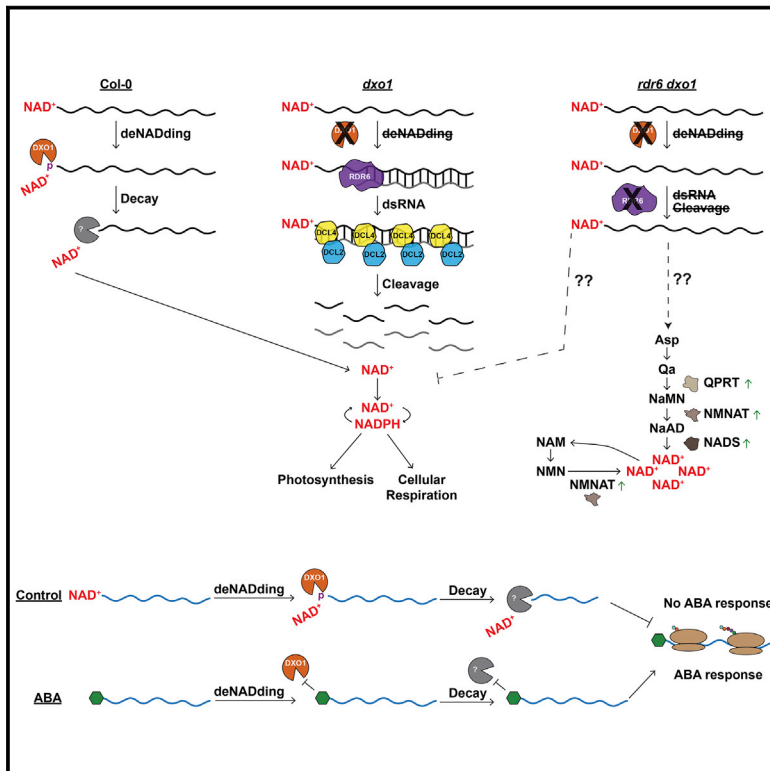


# Developmental Cell

## Messenger RNA 5' NAD<sup>+</sup> Capping Is a Dynamic Regulatory Epitranscriptome Mark That Is Required for Proper Response to Abscisic Acid in Arabidopsis

### Graphical Abstract



### Authors

Xiang Yu, Matthew R. Willmann, Lee E. Vandivier, ..., Eric Lyons, Nathaniel W. Snyder, Brian D. Gregory

### Correspondence

bdgregor@sas.upenn.edu

### In Brief

Eukaryotic RNAs have been found to contain 5'-end NAD<sup>+</sup> caps, but the dynamic nature of these modifications is unknown. Yu et al. demonstrate that plant response to the phytohormone abscisic acid (ABA) reshapes RNA NAD<sup>+</sup> capping to stabilize transcripts encoding ABA response proteins, allowing proper response to this essential phytohormone.

### Highlights

- Messenger RNA NAD<sup>+</sup> capping is widespread and varies between tissues in plants
- NAD<sup>+</sup>-capped RNAs are unstable and a lack of their turnover induces NAD<sup>+</sup> metabolism
- Plant response to abscisic acid (ABA) remodels the NAD<sup>+</sup>-capped transcriptome
- Much of the ABA-mediated NAD<sup>+</sup> transcriptome reprogramming does not require DXO1

Article

# Messenger RNA 5' NAD<sup>+</sup> Capping Is a Dynamic Regulatory Epitranscriptome Mark That Is Required for Proper Response to Abscisic Acid in Arabidopsis

Xiang Yu,<sup>1</sup> Matthew R. Willmann,<sup>2</sup> Lee E. Vandivier,<sup>1,3</sup> Sophie Trefely,<sup>4,5,6</sup> Marianne C. Kramer,<sup>1,3</sup> Jeffrey Shapiro,<sup>1</sup> Rong Guo,<sup>1</sup> Eric Lyons,<sup>7,8</sup> Nathaniel W. Snyder,<sup>6</sup> and Brian D. Gregory<sup>1,3,9,\*</sup>

<sup>1</sup>Department of Biology, University of Pennsylvania, Philadelphia, PA 19104, USA

<sup>2</sup>School of Integrative Plant Science, Cornell University, Ithaca, NY 14853, USA

<sup>3</sup>Cell and Molecular Biology Graduate Group, Perelman School of Medicine, University of Pennsylvania, Philadelphia, PA 19104, USA

<sup>4</sup>Department of Cancer Biology, Perelman School of Medicine, University of Pennsylvania, Philadelphia, PA 19104, USA

<sup>5</sup>Abramson Family Cancer Research Institute, Perelman School of Medicine, University of Pennsylvania, Philadelphia, PA 19104, USA

<sup>6</sup>Center for Metabolic Disease Research, Department of Microbiology and Immunology, Lewis Katz School of Medicine, Temple University, Philadelphia, PA 19140, USA

<sup>7</sup>School of Plant Sciences, University of Arizona, Tucson, AZ 85721, USA

<sup>8</sup>CyVerse, University of Arizona, Tucson, AZ 85721, USA

<sup>9</sup>Lead Contact

\*Correspondence: [bdgregor@sas.upenn.edu](mailto:bdgregor@sas.upenn.edu)

<https://doi.org/10.1016/j.devcel.2020.11.009>

## SUMMARY

Although eukaryotic messenger RNAs (mRNAs) normally possess a 5' end N<sup>7</sup>-methyl guanosine (m<sup>7</sup>G) cap, a non-canonical 5' nicotinamide adenine dinucleotide (NAD<sup>+</sup>) cap can tag certain transcripts for degradation mediated by the NAD<sup>+</sup> decapping enzyme DXO1. Despite this importance, whether NAD<sup>+</sup> capping dynamically responds to specific stimuli to regulate eukaryotic transcriptomes remains unknown. Here, we reveal a link between NAD<sup>+</sup> capping and tissue- and hormone response-specific mRNA stability. In the absence of DXO1 function, transcripts displaying a high proportion of NAD<sup>+</sup> capping are instead processed into RNA-dependent RNA polymerase 6-dependent small RNAs, resulting in their continued turnover likely to free the NAD<sup>+</sup> molecules. Additionally, the NAD<sup>+</sup>-capped transcriptome is significantly remodeled in response to the essential plant hormone abscisic acid in a mechanism that is primarily independent of DXO1. Overall, our findings reveal a previously uncharacterized and essential role of NAD<sup>+</sup> capping in dynamically regulating transcript stability during specific physiological responses.

## INTRODUCTION

The 5' end of eukaryotic mRNAs is co-transcriptionally modified through the addition of a 7-methylguanosine cap (m<sup>7</sup>G), which functions through interaction with various cap-binding proteins to protect mature mRNAs from degradation by 5' to 3' exonucleases (Zhang and Guo, 2017). The m<sup>7</sup>G additionally acts as a unique identifier to regulate nuclear export, polyadenylation, pre-mRNA splicing, and promotes translation initiation of mature mRNAs (Gonatopoulos-Pournatzis and Cowling, 2014). Thus, removal of the cap along with the 3' end polyadenine (polyA) tail are both critical steps for regulating mRNA degradation in eukaryotes. DECAPPING2 (DCP2) is the well-known m<sup>7</sup>G decapping enzyme (Valkov et al., 2016), but eukaryotic genomes encode other enzymes with decapping activity, and much less is known about the functional relevance of these proteins.

Recently, a different type of 5' cap structure, a nicotinamide adenine dinucleotide (NAD<sup>+</sup>) cap has been identified on bacterial RNAs (Chen et al., 2009; Cahová et al., 2015; Bird et al., 2016;

Vvedenskaya et al., 2018; Frindert et al., 2018), yeast RNAs (Walters et al., 2017), mammalian RNAs (Jiao et al., 2017; Bird et al., 2018), and plant RNAs (Wang et al., 2019; Zhang et al., 2019; Kwasnik et al., 2019; Pan et al., 2020). In contrast to the m<sup>7</sup>G cap, the NAD<sup>+</sup> cap promotes degradation of specific transcripts, revealing it as a potential 5' cap-mediated epitranscriptomic regulator. More specifically, the resulting NAD<sup>+</sup>-capped mRNAs are eventually decapped and degraded by the enzyme Rai1/DXO1 (hereafter DXO1) (Jiao et al., 2017).

DXO1 has dual functions, as it can remove the NAD<sup>+</sup> cap through a process called “deNADding” as well as degrade and clear these non-canonically capped transcripts (Xiang et al., 2009; Chang et al., 2012; Jiao et al., 2017). In mammalian cells, DXO1 removes this moiety from NAD<sup>+</sup>-capped transcripts, resulting in free NAD<sup>+</sup> molecules and 5' mono-phosphorylated (5' P) transcripts, and subsequently degrades the resulting 5' P mRNA via its 5'–3' exoribonuclease activity (Jiao et al., 2017; Kiledjian, 2018). In the model plant *Arabidopsis thaliana* (hereafter Arabidopsis), the DXO1 ortholog possesses NAD<sup>+</sup> decapping

activity *in vitro* (Kwasnik et al., 2019; Pan et al., 2020), suggesting that DXO1 is a major regulator of NAD<sup>+</sup>-capped transcripts in mammals and plants. While it is evident that NAD<sup>+</sup> decapping and subsequent RNA removal can regulate mRNA abundance, the physiological relevance of this turnover and whether NAD<sup>+</sup> capping could be a mechanism for dynamic regulation of mRNA stability in response to cellular signals are completely unstudied.

RNA degradation directed by small non-coding RNAs (smRNAs) is an additional RNA turnover mechanism to precisely control mRNA abundance post-transcriptionally. In one such plant pathway, 21–22 nucleotide (nt) smRNAs are generated by DCL cleavage of double-stranded RNAs produced by RNA-dependent RNA polymerase 6 (RDR6) (Willmann et al., 2011). This post-transcriptional gene silencing (PTGS) pathway can be triggered as a secondary control mechanism by exogenous RNAs when canonical RNA surveillance pathways are absent and/or normal RNA processing is impaired (Baulcombe, 1996; Liu and Chen, 2016). In fact, losing the function of DCP2, cap-binding proteins (e.g., CBP80/ABH1) or EXORIBONUCLEASE 4 (XRN4) can induce these PTGS pathways (Gregory et al., 2008; Martínez de Alba et al., 2015; Zhang et al., 2015), suggesting they are backup mechanisms to tightly control mRNA abundance. Recently, it was also demonstrated that loss of DXO1 function resulted in PTGS-mediated smRNA processing from over 1,000 protein-coding mRNAs in Arabidopsis (Kwasnik et al., 2019; Pan et al., 2020). However, the significance of this smRNA processing is unclear, since their presence does not contribute to developmental defects of *dxo1* mutant plants (Kwasnik et al., 2019; Pan et al., 2020).

Abscisic acid (ABA) is a major plant hormone that is involved in responses to many environmental stresses and controls the transition of seeds from dormancy to germination (Finkelstein, 2013). In fact, impairment of m<sup>7</sup>G cap recognition and decapping, as well as RNA degradation, alter plant sensitivity to ABA and abiotic stresses by regulating the biosynthesis, signal transduction, and expression of downstream ABA-responsive genes (Hugouvieux et al., 2001; Wawer et al., 2018). While the importance of regulating removal of the canonical m<sup>7</sup>G cap in ABA response is evident, whether decapping of the non-canonical 5' NAD<sup>+</sup> cap is important for response to ABA has not been explored.

Here, we use a variant of NAD-capture sequencing (Cahová et al., 2015) in combination with degradome and RNA sequencing (RNA-seq) to identify NAD<sup>+</sup>-capped RNAs in Arabidopsis unopened flower buds, and during seedling response to the phytohormone ABA, and examine the role of this moiety in regulating mRNA stability. This analysis reveals that RNA NAD<sup>+</sup> capping is widespread and varies between plant tissues to destabilize specific subsets of the transcriptome when they are not required. Our findings also illuminate a previously uncharacterized mechanism in which mRNA NAD<sup>+</sup> caps can be dynamically regulated to affect a eukaryotic physiological response.

## RESULTS

### DXO1 Acts as an Eraser of RNA 5' End NAD<sup>+</sup> Caps in Arabidopsis

AtDXO1 (AT4G17620) is the single copy Arabidopsis ortholog of mammalian DXO1 (Figure S1A). According to available data (Kle-

pikova et al., 2016), the *DXO1* transcript is highly abundant in roots, young leaves, inflorescence shoot apex, flower buds, and dry seeds, suggesting the importance of DXO1 to Arabidopsis development (Figure S1B). To test this, we obtained two independent *DXO1* mutant alleles, *dxo1-1* and *dxo1-2* (Figure S1C). Supporting our hypothesis and previous findings (Kwasnik et al., 2019; Pan et al., 2020), both *dxo1* mutant alleles display severe developmental defects as compared with wild-type Columbia-0 (hereafter Col-0) plants. In fact, 2-week-old *dxo1* mutant seedlings showed dwarfism and yellow coloration (Figure S1D), 3-week-old *dxo1* plants displayed growth delays as measured by a decrease in leaf number (Figure S1E), and flowering *dxo1* mutant plants were significantly less fertile with much shorter siliques (Figure S1F). Arabidopsis transgenic lines expressing the fusion protein of DXO1 and  $\beta$ -glucuronidase (GUS) in the *dxo1-2* mutant background rescued the mutant phenotype, indicating that loss of *DXO1* results in the aberrant phenotypes observed (Figure S1G). Additionally, GUS staining revealed that DXO1 is highly abundant in shoot and root apices (Figure S1H). To determine the subcellular localization of DXO1, we generated transgenic lines in the *dxo1-2* mutant background expressing eGFP-tagged *DXO1* and found that DXO1 is localized to both the nucleus and cytoplasm in protoplasts and root tips (Figures S1I and S1J). These results reveal that DXO1 is localized throughout the cell and plays critical functions in both vegetative and reproductive developmental processes, displaying its importance to plant biology.

While previous studies demonstrated that DXO1 functions in the decapping of RNA 5' end NAD<sup>+</sup> caps *in vitro* (Kwasnik et al., 2019), whether it has the same function *in vivo* is unknown. To test this, we performed NAD-capture sequencing with the slight variation that full NAD<sup>+</sup>-capped transcripts were used as the substrate in RNA sequencing library preparation (hereafter NAD-seq) (Cahová et al., 2015; Zheng et al., 2010; Li et al., 2012; Figure S2A). To begin, we validated the NAD<sup>+</sup> capture approach using *in vitro* synthesized luciferase (LUC) transcripts with and without the addition of a NAD<sup>+</sup> cap followed by RT-qPCR. As expected, we captured only NAD<sup>+</sup> modified LUC transcripts after ADP-ribosylcyclase (ADPRC) treatment compared with unmodified LUC transcripts (Figure S2B). With this proof of principle, we performed NAD-seq in two biological replicates of Col-0 and *dxo1-2* mutant unopened flower buds (Figures S1B and S1F). In tandem, we performed total RNA-seq for these same samples to serve as a background for identifying NAD<sup>+</sup>-capped transcripts. The resulting NAD-seq and RNA-seq libraries were sequenced and provided ~11–20 million mapped reads per library. The biological replicates of each library type from the distinct genotypes clustered together (Figures S2C and S2D), indicating the high quality and reproducibility of these libraries.

Similar to studies in mammalian cells (Jiao et al., 2017), we found a significant ( $p$  value < 0.001, Chi-squared test) increase in the ratio of reads uniquely mapping to mRNAs as compared with rRNAs in *dxo1-2* mutants compared with Col-0 libraries (Figure S2E), indicating that NAD<sup>+</sup>-capped mRNAs were enriched in the absence of DXO1 function. Using these datasets, we calculated the NAD<sup>+</sup>-capped proportion ( $\log_2[\text{RPM}_{\text{NAD-seq}}/\text{RPM}_{\text{RNA-seq}}]$ ) for each transcript in Col-0 and *dxo1-2* mutants, and found a significantly ( $p$  value < 0.001, Mann-Whitney  $U$

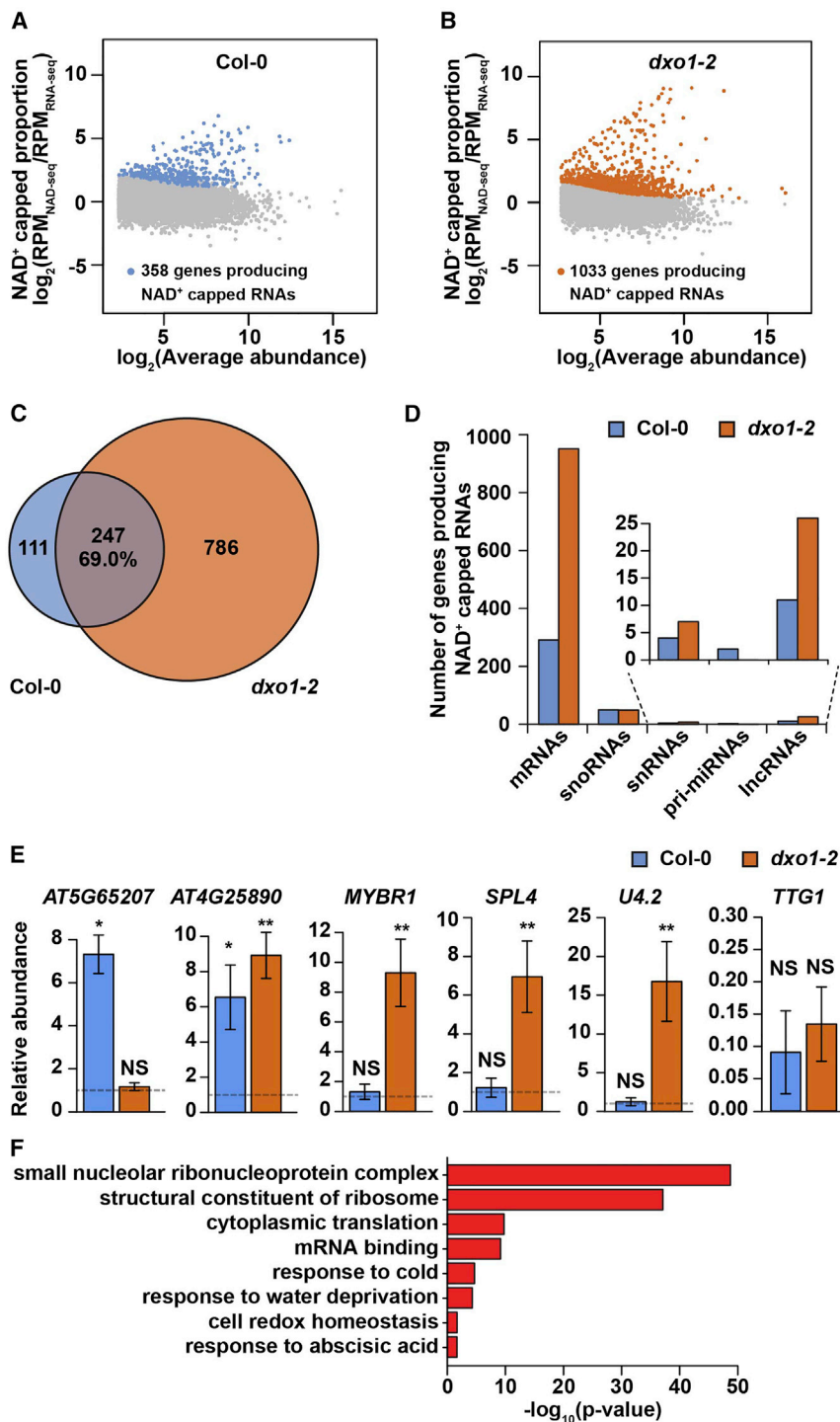


**Figure 1. NAD-Seq Reveals that DXO1 Functions as a deNADding Enzyme In Planta**

(A and B) MA plots showing genes producing NAD<sup>+</sup>-capped RNAs enriched in Col-0 (A) (blue) and *dxo1-2* mutant (B) (orange) unopened flower buds.

(C) The overlap of genes producing NAD<sup>+</sup>-capped RNAs identified in Col-0 (blue) and *dxo1-2* mutant (orange) unopened flower buds.

(D) The number of genes producing NAD<sup>+</sup>-capped RNAs encoding mRNAs, snoRNAs, snRNAs, pri-miRNAs, and lncRNAs in Col-0 (blue bars) and *dxo1-2* mutant (orange bars) unopened flower buds.

(E) The relative abundance of *AT5G65207*, *AT4G25890*, *MYBR1*, *SPL4*, *U4.2*, and *TTG1* in NAD<sup>+</sup>-captured RNA samples as compared to total RNA samples containing *in vitro* transcribed NAD<sup>+</sup> LUC as a spike-in control. The dashed lines indicate the average abundance of the indicated transcripts in total RNA samples normalized to NAD<sup>+</sup> LUC as a spike-in control. NS denotes no significance, while \* and \*\* denote p value < 0.05 and 0.01, respectively, Student's t test. Error bars indicate  $\pm$  standard error of the mean.

(F) The enriched GO terms for 1,033 DXO1 deNADding targets ordered by  $-\log_{10}(p \text{ value})$ .

referred to as NAD<sup>+</sup>-capped transcripts) identified in Col-0 (247; 69%) were also identified in the *dxo1-2* plants, while an additional 786 were found only in the absence of DXO1 function (Figure 1C). These 786 NAD<sup>+</sup>-capped transcripts were likely not detected in Col-0 because their NAD<sup>+</sup> cap was efficiently removed by DXO1. In agreement with prior data (Jiao et al., 2017), the majority of NAD<sup>+</sup>-capped transcripts identified in the *dxo1-2* mutant, and thus, dependent on DXO1 function for their deNADding, are protein-coding mRNAs (951; 92.1%) and small nucleolar RNAs (snoRNAs; 49; 4.7%) (Figure 1D; Table S1). We also identified 26 long non-coding RNAs (lncRNAs) and seven small nuclear RNAs (snRNAs) with NAD<sup>+</sup> caps, indicating that NAD<sup>+</sup> caps can be added to a variety of transcripts (Figure 1D). To validate these results, we performed NAD capture followed by quantitative PCR for five randomly selected NAD<sup>+</sup>-capped transcripts (one NAD<sup>+</sup>-capped only in Col-

test) increased level of proportion NAD<sup>+</sup> capping in the transcriptome of *dxo1* mutant as compared with Col-0 (Figure S2F), indicating that DXO1 is also a plant deNADding enzyme. Using this statistic, we were also able to identify 358 and 1,033 genes producing significantly (FDR < 0.1, DESeq2) high proportion NAD<sup>+</sup>-capped values in Col-0 and *dxo1-2* unopened flower buds, respectively (Figures 1A and 1B; Tables S1 and S2). Most of the genes producing NAD<sup>+</sup>-capped transcripts (hereafter also

referred to as NAD<sup>+</sup>-capped transcripts) identified in Col-0 (247; 69%) were also identified in the *dxo1-2* plants, while an additional 786 were found only in the absence of DXO1 function (Figure 1C). These 786 NAD<sup>+</sup>-capped transcripts were likely not detected in Col-0 because their NAD<sup>+</sup> cap was efficiently removed by DXO1. In agreement with prior data (Jiao et al., 2017), the majority of NAD<sup>+</sup>-capped transcripts identified in the *dxo1-2* mutant, and thus, dependent on DXO1 function for their deNADding, are protein-coding mRNAs (951; 92.1%) and small nucleolar RNAs (snoRNAs; 49; 4.7%) (Figure 1D; Table S1). We also identified 26 long non-coding RNAs (lncRNAs) and seven small nuclear RNAs (snRNAs) with NAD<sup>+</sup> caps, indicating that NAD<sup>+</sup> caps can be added to a variety of transcripts (Figure 1D). To validate these results, we performed NAD capture followed by quantitative PCR for five randomly selected NAD<sup>+</sup>-capped transcripts (one NAD<sup>+</sup>-capped only in Col-

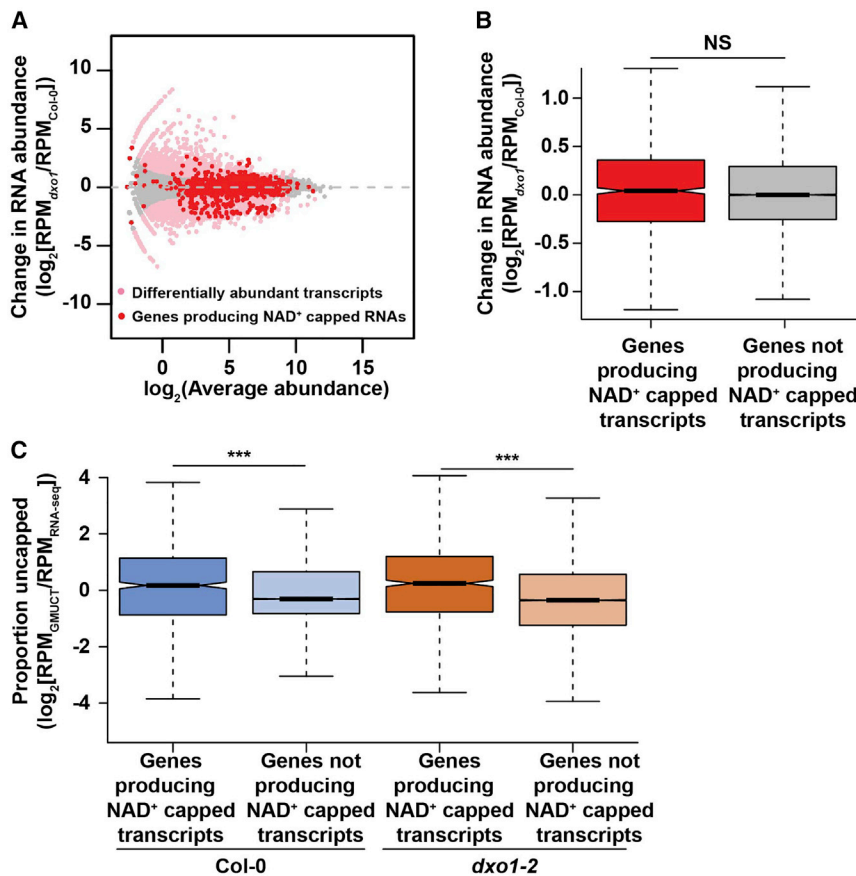


**Figure 2. DXO1 Functions in NAD<sup>+</sup> Decapping-Directed RNA Turnover**

(A) MA plot showing differentially abundant transcripts (pink, FDR < 0.05) between Col-0 and *dxo1* mutant unopened flower buds. Red indicates genes producing NAD<sup>+</sup>-capped mRNAs in *dxo1* plants (N = 951).

(B) The fold change of RNA abundance ( $\log_2[\text{RPM}_{dxo1}/\text{RPM}_{Col-0}]$ ) for genes producing NAD<sup>+</sup>-capped mRNAs (N = 951) and those without a NAD<sup>+</sup> cap (N = 26,465). NS denotes no significance, Mann-Whitney U test.

(C) The proportion uncapped value of genes producing transcripts with a NAD<sup>+</sup> cap and those without a NAD<sup>+</sup> cap in Col-0 (dark and light blue, respectively) and *dxo1* mutant (dark and light orange, respectively) plants. \*\*\* denotes p value < 0.001, Mann-Whitney U test.

proteins functioning in reducing or oxidizing NAD<sup>+</sup>/NADH for post-transcriptional regulation. In total, our findings reveal that DXO1 is an *in vivo* NAD<sup>+</sup> decapping enzyme, and this modification is added to a specific set of transcripts in plant unopened flower buds.

### Arabidopsis DXO1 Functions in deNADding-Mediated RNA Turnover

We investigated the transcriptome changes that occur in the absence of

DXO1 function. To do this, we performed polyA<sup>+</sup> RNA sequencing (mRNA-seq) in unopened flower buds from two biological replicates of Col-0 and one biological replicate for each *dxo1* mutant allele to act as biological replicates of each other given their similar phenotypes, which produced ~11–19 million mapped reads per library. The biological replicates from the both *dxo1* mutant alleles clustered together and were distinct from those for Col-0 (Figure S3A), indicating the high quality and reproducibility of these libraries. Using edgeR (Robinson et al., 2010), we identified 1,230 and 1,506 transcripts that were significantly more and less abundant, respectively, in the *dxo1* mutant as compared with Col-0 plants (Figure 2A). To determine if the transcript abundance for NAD<sup>+</sup>-capped RNAs changed in the absence of DXO1, we focused on the 951 protein-coding transcripts that are dependent on DXO1 for their decapping (Figure 1C). The abundance of these transcript populations did not significantly change in *dxo1* mutants compared with Col-0 (Figures 2A and 2B), nor was the RNA abundance for NAD<sup>+</sup>-capped transcripts significantly different than those not producing these modified RNAs (Figure 2B). Thus, the presence of a NAD<sup>+</sup> cap does not affect their overall level of abundance in the *dxo1* mutant plants (Figure 2A), suggesting additional post-transcriptional control of these RNAs.

To determine if NAD<sup>+</sup> capping affects transcript stability, we performed genome-wide mapping of uncapped and cleaved transcripts (GMUCT) (Gregory et al., 2008; Willmann et al., 2014) to quantify the degradation and cleaved intermediates of

spike-in control specifically in *dxo1-2* mutant plants. In further support of the NAD-seq findings, *AT5G65207* and *AT4G25890* displayed NAD<sup>+</sup>-capped transcript enrichment (p value < 0.05, Student's t test) specifically in Col-0 and both genotypes, respectively (Figure 1E), while the negative control *TTG1* displayed no enrichment in either genotype (relative abundance < 0) (Figure 1E). Overall, our NAD-seq results reveal that DXO1 functions *in vivo* as a deNADding enzyme that primarily targets protein-coding mRNAs but can also remove this modification from various non-coding RNAs.

We performed gene ontology (GO) enrichment analysis using the database for annotation, visualization, and integrated data (DAVID) (Huang et al., 2009) on the 1,033 DXO1 deNADding targets to characterize the biological processes that were likely regulated by NAD<sup>+</sup> capping (Figures 1B–1D). NAD<sup>+</sup>-capped transcripts were enriched for those encoding proteins involved in cytoplasmic translation and mRNA binding, as well as numerous abiotic stress responses, including response to cold, water deprivation, and ABA (Figure 1F). They were also highly enriched for mRNAs encoding proteins involved in cell redox homeostasis (Figure 1F), a process where free NAD<sup>+</sup> is an essential cofactor for redox coupling in all living cells (Xiao et al., 2018). Using the MapMan tool (Thimm et al., 2004), we took a closer look at what transcripts are NAD<sup>+</sup>-capped in this GO term and found that those in this functional class encode thioredoxin proteins, one class of redox proteins (Figure S2G). Thus, there may be a feedback mechanism wherein NAD<sup>+</sup> caps tag transcripts encoding redox

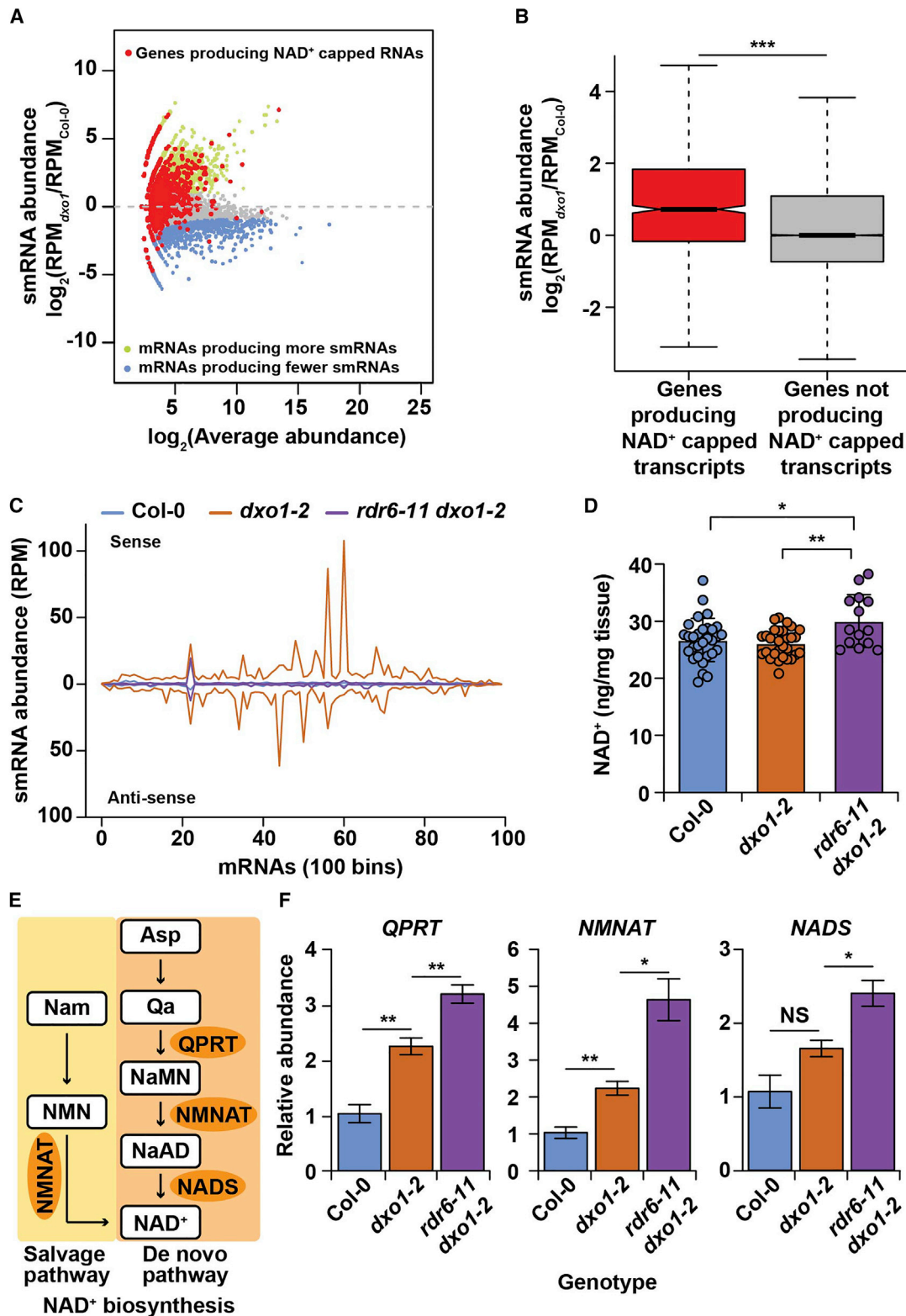


**Figure 3. NAD<sup>+</sup>-Capped Transcripts are Targeted by RDR6-Mediated PTGS in the Absence of DXO1**

(A) MA plot showing mRNAs that produce significantly (adjusted p value < 0.05) more (green) and less (blue) smRNAs in *dxo1* mutants compared with Col-0. Red dots highlight mRNAs with a NAD<sup>+</sup> cap (N = 951).

(legend continued on next page)

polyA<sup>+</sup> transcripts in the same samples used for mRNA-seq. The Col-0 GMUCT libraries have been previously analyzed and described (Willmann et al., 2014), while the resulting *dxo1* mutant GMUCT libraries were sequenced and provided ~25 and 35 million mapped reads in the two libraries. The biological replicates from both *dxo1* mutant alleles clustered together and were distinct from Col-0, indicating the high quality and reproducibility of the GMUCT libraries (Figure S3B). Using the GMUCT and mRNA-seq data, we measured the relative stability of transcripts using the proportion uncapped metric ( $\log_2[\text{RPM}_{\text{GMUCT}}/\text{RPM}_{\text{RNA-seq}}]$ ) (Vandivier et al., 2015; Anderson et al., 2018), where a higher value correlates with a less stable transcript and vice versa.

We first compared the proportion uncapped for NAD<sup>+</sup>-capped transcripts to those that lack this modification in Col-0 and *dxo1* mutant plants. As expected, we found that NAD<sup>+</sup>-capped transcripts display a significantly ( $p$  value < 0.001, Mann-Whitney U test) higher proportion of uncapped value (less stable) than those that lack this modification in Col-0, revealing that, similar to in mammals (Jiao et al., 2017), these RNAs tend to be unstable (Figure 2C). We also observed that the stability of these transcripts is unchanged in *dxo1* mutants, as transcripts with a high proportion of NAD<sup>+</sup> capping are significantly ( $p$  value < 0.001, Mann-Whitney U test) less stable than those without a NAD<sup>+</sup> cap, and their proportion uncapped values were similar between Col-0 and *dxo1* mutants (Figure 2C). This indicates that while DXO1 is required for decapping of these transcripts, there is an additional pathway for destabilizing of NAD<sup>+</sup>-capped transcripts when this enzyme is non-functional.

### NAD<sup>+</sup>-Capped Transcripts Are Processed into Small RNAs in the Absence of DXO1 Function

Since we observed that NAD<sup>+</sup>-capped transcripts are unstable even in *dxo1* mutant plants, it is likely that there is an additional mechanism to destabilize them when DXO1 function is absent. Prior studies revealed that an accumulation of transcripts with non-canonical 5' ends can trigger their processing into smRNAs through RDR6-dependent PTGS (Herr et al., 2006; Martínez de Alba et al., 2015; Gregory et al., 2008; Zhang et al., 2015). Thus, we hypothesized that the accumulation of NAD<sup>+</sup>-capped transcripts in *dxo1* mutant plants (Figures 1B and 1C) could trigger degradation through PTGS. To test this, we performed small RNA sequencing (smRNA-seq) using the same samples as for mRNA-seq, which produced ~11–40 million mapped reads per library. The biological replicates from both *dxo1* mutant alleles clustered together and were distinct from Col-0, indicating the high quality and reproducibility of the libraries (Figure S4A). We found that 21 and 22 nt smRNAs derived from both

strands of protein-coding transcripts accumulated in *dxo1* mutant compared with Col-0 plants (Figures 3A and S4B–S4D).

In total, 2,337 and 1,282 mRNAs produced significantly (adjusted  $p$  value < 0.05, edgeR) more and less 21–22 nt smRNAs, respectively, in *dxo1* mutants compared with Col-0 plants, (Figure 3A; Table S3). Additionally, we found that NAD<sup>+</sup>-capped transcripts in *dxo1* mutant flower buds (Figure 1B) produced significantly ( $p$  value < 0.001, Mann-Whitney U test) more 21–22 nt smRNAs than those without NAD<sup>+</sup> caps (Figures 3A and 3B). In fact, when the collection of NAD<sup>+</sup>-capped transcripts was separated into quartiles based on their increasing NAD<sup>+</sup>-capped proportion values (quartile 1 lowest and 4 highest), we observed significant (all  $p$  values < 0.05, Mann-Whitney U test) monotonic increases in the levels of smRNAs produced in *dxo1* mutant compared with Col-0 flower buds. For example, two NAD<sup>+</sup>-capped transcripts, *AT4G18670* and *AT2G45470*, accumulated significantly ( $p$  value < 0.001, Student's  $t$  test) higher levels of 21–22 nt smRNAs from both their sense and antisense strands in *dxo1* mutant compared with Col-0 plants (Figures S4B and S4C), suggesting RDR6 is involved in their biogenesis. Our findings reveal that NAD<sup>+</sup>-capped transcripts are processed into smRNAs in the absence of DXO1 function (Figures 3A, 3B, and S4B–S4E), providing a mechanism to keep their levels of stability and total abundance similar to those in Col-0 plants (Figure 2).

As NAD<sup>+</sup>-capped transcripts appear to be targeted for RDR6-dependent PTGS in the absence of DXO1, we tested this by crossing a null mutation of RDR6 (*rdr6-11*) into the *dxo1-2* mutant background, resulting in plants that have lost the function of both RDR6 and DXO1 simultaneously (*rdr6-11 dxo1-2*). We then tested if this PTGS pathway was responsible for the processing of smRNAs from NAD<sup>+</sup>-capped transcripts in the absence of DXO1 by performing smRNA-seq in unopened flower buds from the *rdr6-11 dxo1-2* double mutants (Figure S4A). We found that smRNAs processed from these transcripts were reduced to levels similar to those in Col-0 in the *rdr6-11 dxo1-2* double mutant plants (Figure 3C), indicating that RDR6 is required for the biogenesis of smRNAs from NAD<sup>+</sup>-capped transcripts in the absence of DXO1 mutant function. We also found that the impairment of RDR6 function did not rescue the morphological defects observed in *dxo1* mutant plants, as *dxo1* single and *rdr6-11 dxo1-2* double mutant plants displayed identical phenotypes (Figure S4F), consistent with previous reports (Kwasnik et al., 2019; Pan et al., 2020). These findings suggest that plant cells might use smRNA biogenesis as an RNA degradation pathway for NAD<sup>+</sup>-capped transcripts in the absence of DXO1 function, but this hypothesis needs further exploration.

(B) Fold change of 21–22 nt smRNA abundance from DXO1-regulated mRNAs with NAD<sup>+</sup> caps ( $N = 951$ ) and mRNAs without NAD<sup>+</sup> caps ( $N = 26,258$ ) in *dxo1* mutants as compared with Col-0. \*\*\* denotes  $p$  value < 0.001, Mann-Whitney U test.

(C) The distribution of 21–22 nt smRNAs along both strands of mRNAs with a significant proportion of NAD<sup>+</sup> capping in Col-0 (blue), *dxo1* single (orange), and *rdr6-11 dxo1-2* double mutant (purple) unopened flower buds. Signal above/below the 0 line indicates the reads (RPM) mapped to the sense/antisense strand of the mRNAs.

(D) Quantification of total NAD<sup>+</sup> levels in Col-0 (blue), *dxo1-2* single (orange), and *rdr6-11 dxo1-2* double mutant (purple) 21-day-old seedlings. Dots indicate individual biological replicates. Error bars indicate  $\pm$  standard error of the mean.

(E) A schematic diagram illustrating the key steps of *de novo* (orange background) and salvage pathways (yellow background) for NAD<sup>+</sup> biosynthesis in plants.

(F) The relative abundance of transcripts encoding NAD<sup>+</sup> biosynthesis proteins *QPRT*, *NMNAT*, and *NADS* in Col-0 (blue), *dxo1-2* (orange), and *rdr6-11 dxo1-2* (purple). The values are normalized to those for Col-0 and the *ACT1* transcript as an internal control. Error bars indicate  $\pm$  standard error of the mean.

(D and F) NS denotes no significance. \* and \*\* denote  $p$  value < 0.05 and 0.01, respectively, Student's  $t$  test.

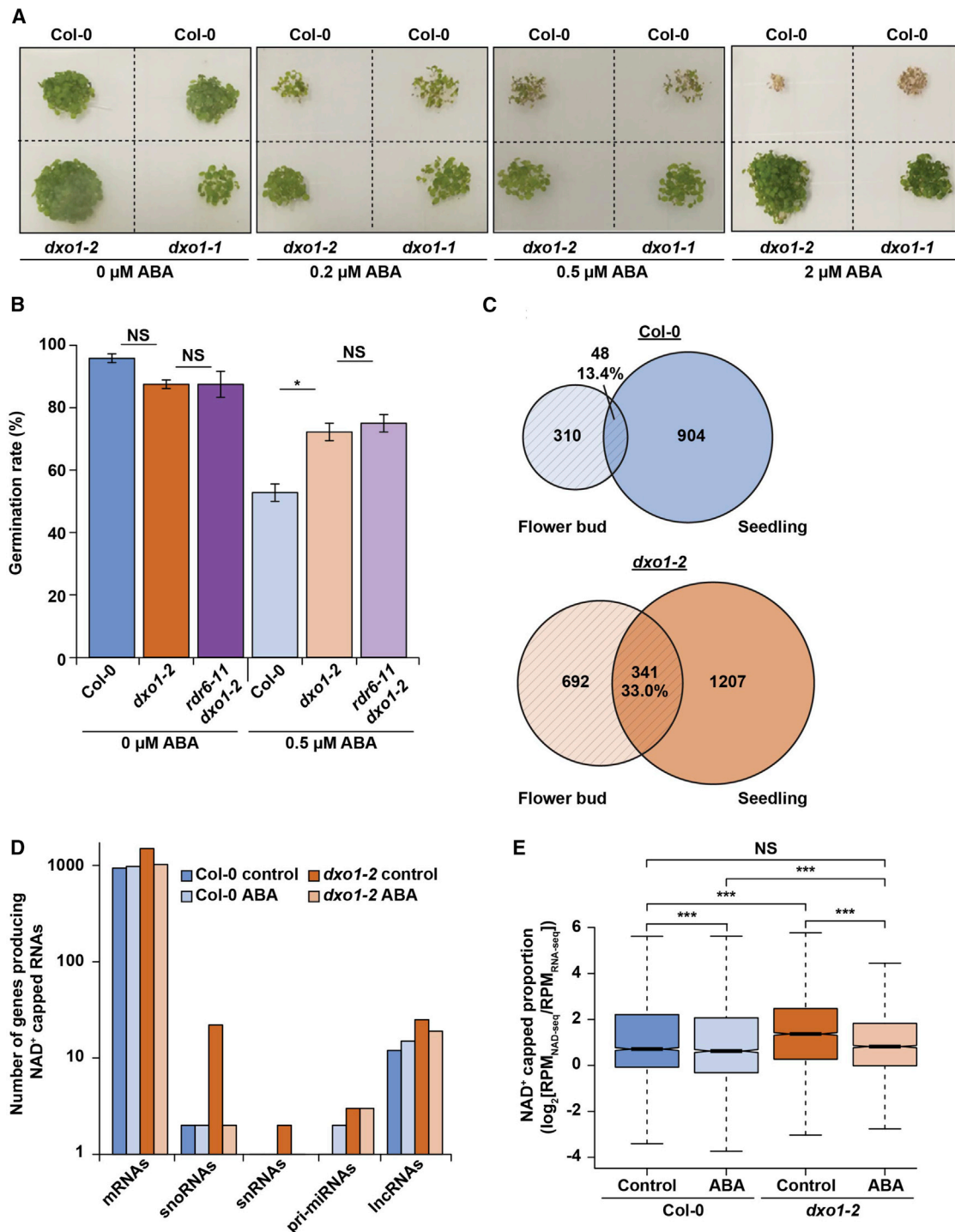


**Figure 4. DXO1 Is Required for Proper ABA Response, and This Plant Hormone Remodels the NAD<sup>+</sup> Capped Transcriptome**

(A) Representative images of seed germination of Col-0, *dxo1-1*, and *dxo1-2* 7-day-old seedlings with 0, 0.2, 0.5, and 2 μM ABA.

(B) Seed germination rate of Col-0 (blue bars), *dxo1-2* single (orange bars), and *rdr6-11 dxo1-2* double (purple bars) mutant 4-day-old seedlings with 0 μM (dark colors) and 0.5 μM ABA (shaded colors). Error bars indicate ± standard error of the mean. NS denotes no significance, and \* denotes p value < 0.05, respectively, Student's t test.

(C) The overlap of NAD<sup>+</sup>-capped RNAs identified in unopened flower buds (light striped colors) or 12-day-old seedlings (dark colors) of Col-0 (blue circles) and *dxo1-2* (orange circles), respectively.

(legend continued on next page)

NAD<sup>+</sup> is a ubiquitous coenzyme in eukaryotic cell redox reactions. Thus, the NAD<sup>+</sup> cap modification on mRNA transcripts provides a potential link between NAD<sup>+</sup> metabolism and post-transcriptional regulation (Figures 1D and S2F; Kiledjian, 2018). We hypothesized that loss of DXO1 decapping function would result in NAD<sup>+</sup> being trapped on mRNAs, and thus, lead to increased NAD<sup>+</sup> biogenesis to restore free NAD<sup>+</sup> levels. To test this, we performed quantitative liquid chromatography-high resolution mass spectrometry (LC-HRMS) (Frederick et al., 2017) to measure global levels of free NAD<sup>+</sup> in Col-0 and *dxo1-2* single mutant seedlings. We found that there was no significant difference in the total NAD<sup>+</sup> levels between Col-0 and *dxo1* single mutant plants, indicating that loss of DXO1 does not increase total NAD<sup>+</sup> levels (Figure 3D). Given that RDR6-dependent PTGS targets NAD<sup>+</sup>-capped RNAs in the absence of DXO1, we measured NAD<sup>+</sup> levels in *rdm6-11 dxo1-2* plants. We found that total NAD<sup>+</sup> levels were significantly (*p* values < 0.05, Student's *t* test) increased in *rdm6-11 dxo1-2* double mutant plants as compared with both Col-0 and *dxo1-2* single mutant plants (Figure 3D). This increase suggests that when NAD<sup>+</sup> cannot be removed from mRNAs in the absence of both DXO1-mediated decapping and RDR6-directed smRNA processing of NAD<sup>+</sup>-capped transcripts, plants increase total NAD<sup>+</sup> levels.

In plants, the NAD<sup>+</sup> biosynthesis pathways include *de novo* and salvage pathways (Hashida et al., 2009). The *de novo* pathway requires several enzymes, including quinolinate phosphoribosyltransferase (QPRT), nicotinate/nicotinamide mononucleotide adenyltransferase (NMNAT), and NAD<sup>+</sup> synthetase (NADS) to convert aspartate to NAD<sup>+</sup>, while NMNAT is common to both pathways (Hashida et al., 2009) (Figure 3E). To test if the levels of mRNAs encoding these enzymes increase in response to a lack of NAD<sup>+</sup> cap removal, we examined the abundance of the transcripts encoding these three enzymes using RT-qPCR and found that transcripts encoding the first two proteins required for NAD<sup>+</sup> biosynthesis (QPRT and NMNAT) were both significantly (*p* values < 0.01, Student's *t* test) more abundant in *dxo1-2* single and *rdm6-11 dxo1-2* double mutant plants as compared with Col-0 (Figure 3F). Notably, the double mutant had significantly (*p* values < 0.05, Student's *t* test) higher levels of both mRNAs compared with *dxo1-2* single mutants (Figure 3F). The transcript encoding the final enzyme required for NAD<sup>+</sup> biosynthesis (NADS) was significantly (*p* value < 0.05, Student's *t* test) more abundant only in *rdm6-11 dxo1-2* double mutant plants as compared with both Col-0 and *dxo1-2* single mutants (Figure 3F). These results indicate that when NAD<sup>+</sup>-capped RNAs are not decapped by DXO1 or processed into RDR6-dependent smRNAs, transcripts encoding the proteins required for the final stage of the salvage and the last three steps of *de novo* NAD<sup>+</sup> biosynthesis are specifically increased.

### DXO1 Is Required for Proper Plant Response to ABA during Seed Germination

We found that a collection of DXO1-dependent NAD<sup>+</sup>-capped mRNAs were enriched in those encoding proteins involved in the plant response to ABA (Figure 1E), so we hypothesized

that DXO1 function may be required for proper plant response to ABA during seed germination. We measured the germination efficiency of Col-0 and both mutant alleles of *dxo1* with increasing concentrations of ABA (0, 0.2, 0.5, and 2 μM). As expected, Col-0 seed germination was sensitive to increasing ABA levels, as fewer seeds germinated in a concentration-dependent manner (Figure 4A). Conversely, *dxo1* mutant seeds were insensitive to the varying ABA concentrations, as they continued germinating in the presence of increasing ABA levels compared with Col-0 (Figure 4A). In fact, *dxo1* mutant seeds were able to germinate when the ABA concentration was as high as 10 μM (Figure S5A), indicating the importance of DXO1 for proper ABA response during plant seed germination.

Given the role of RDR6-dependent smRNA processing in NAD<sup>+</sup>-capped transcript destabilization, we measured seed germination for Col-0, *dxo1-2* single, and *rdm6-11 dxo1-2* double mutant plants without and with 0.5 μM ABA. We found that *dxo1-2* single and *rdm6-11 dxo1-2* double mutant seeds both displayed similar ABA insensitivity as compared with Col-0 upon exposure to increased ABA levels (Figure 4B). These results indicate that both the developmental defects and insensitivity to ABA seed germination inhibition of *dxo1-2* plants is not a result of the PTGS-mediated smRNA processing of NAD<sup>+</sup>-capped mRNAs.

### Exposure to ABA Leads to Global Remodeling of the NAD<sup>+</sup>-Capped Transcriptome

We next set out to determine the effect of this hormone on the NAD<sup>+</sup>-capped transcriptome. To examine this, we performed NAD-seq and total RNA-seq on 12-day-old Col-0 and *dxo1* seedlings treated without and with 0.5 μM ABA, producing ~14–22 million total reads per library. The biological replicates of each library type from the distinct genotypes and treatments clustered together (Figures S5B and S5C), indicating the high quality and reproducibility of our libraries. In Col-0 seedlings, we detected 952 and 995 genes producing NAD<sup>+</sup>-capped transcripts under control and 0.5 μM ABA conditions, respectively. In *dxo1* mutant seedlings, we identified 1,548 and 1,048 genes producing NAD<sup>+</sup>-capped transcripts under control and 0.5 μM ABA conditions, respectively (Tables S4, S5, S6, and S7). To interrogate the developmental specificity of NAD<sup>+</sup> capping in the Arabidopsis transcriptome, we compared NAD<sup>+</sup>-capped transcripts between unopened flower buds and 12-day-old seedlings in both Col-0 and *dxo1* mutants. We found that only 13.4% and 33% of NAD<sup>+</sup>-capped transcripts in flower buds from Col-0 and *dxo1* single mutants, respectively, were also detected in seedlings of these same genotypes (Figure 4C), indicating NAD<sup>+</sup> capping is indeed regulated in a developmental-specific manner.

As for unopened flower buds, the majority of NAD<sup>+</sup>-capped transcripts detected in 12-day-old seedlings were protein-coding mRNAs in both conditions (± ABA). Additionally, we also detected some NAD<sup>+</sup>-capped pri-miRNAs, snoRNAs, and other lncRNAs in these younger plant tissues (Figure 4D; Tables S4, S5, S6, and S7). Notably, there were more snoRNAs with a significant NAD<sup>+</sup>-capped proportion value present in 12-day-old

(D) The number of genes producing NAD<sup>+</sup>-capped transcripts identified in Col-0 and *dxo1-2* mutant 12-day-old seedlings both without and with 0.5 μM ABA treatment for the different specified categories.

(E) NAD<sup>+</sup>-capped proportion for Col-0 and *dxo1-2* mutant 12-day-old seedlings without and with 0.5 μM ABA treatment. \*\*\* denotes *p* value < 0.001 and NS denotes no significance, Mann-Whitney U test.

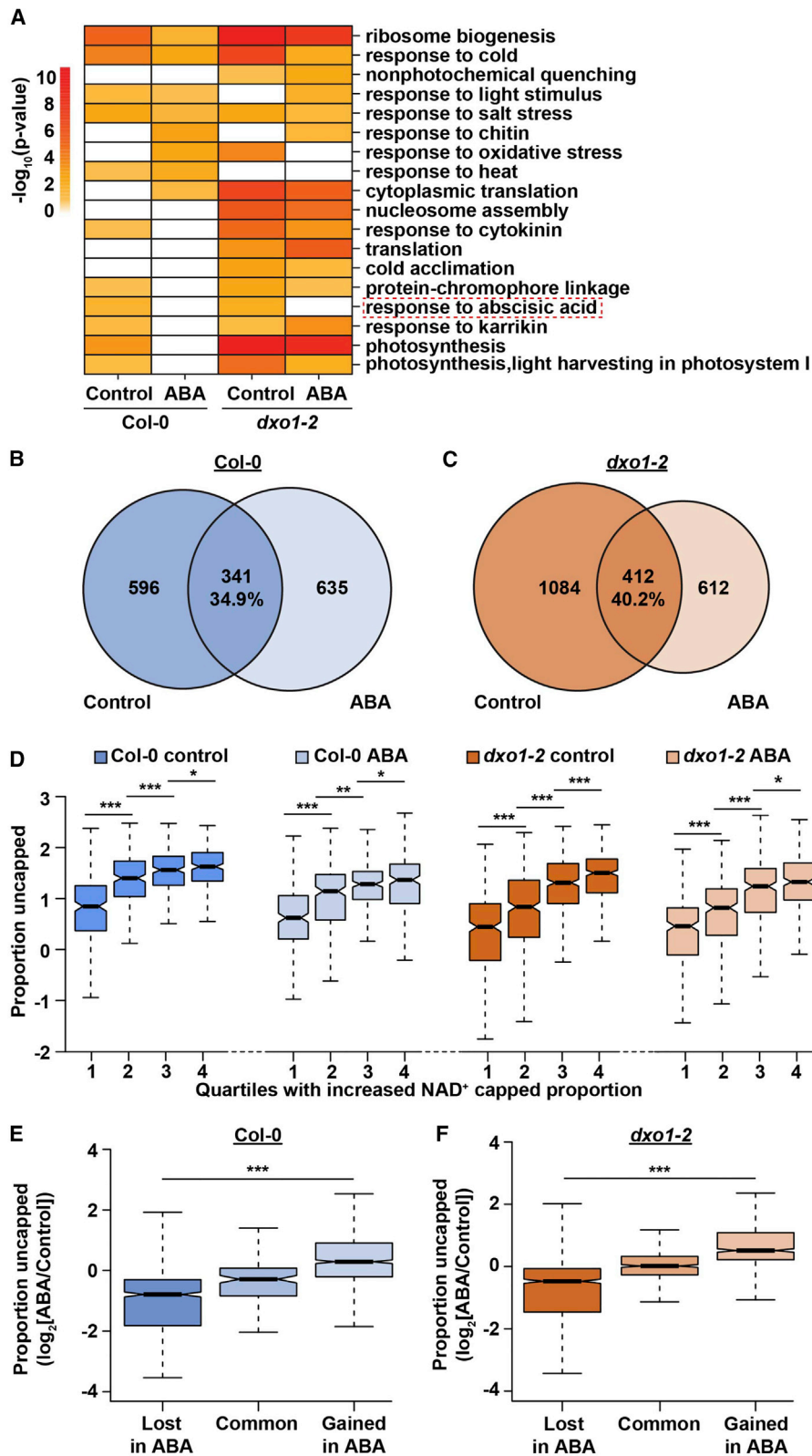


**Figure 5. ABA Response Directs Dynamic Changes in mRNA NAD<sup>+</sup> Capping to Affect the Stability of Specific Transcripts**

(A) The list of biological process GO terms that are enriched ( $p$  value  $< 0.01$ ) in at least two of the four indicated conditions. The color bar indicates the  $-\log_{10}(p$  value) of the enrichment for that condition. White boxes indicate no enrichment.

(legend continued on next page)

*dxo1* seedlings compared with Col-0 under control conditions (Figure 4C), which was different than in the unopened flower buds, where snoRNAs were also present in Col-0 (Figure 1D). In fact, this class of NAD<sup>+</sup>-capped transcripts were reduced to Col-0 levels (mostly disappeared) in *dxo1* mutant seedlings upon 0.5 μM ABA treatment. Additionally, some pri-miRNA transcripts were also modified with a NAD<sup>+</sup> cap. In both Col-0 and *dxo1* seedlings, we identified NAD<sup>+</sup>-capped primary *MIR167D*, *MIR167A*, *MIR158A*, and *MIR398C*, but their levels of NAD<sup>+</sup> capping and treatment under which this modification occurred varied for these RNAs (Figure S5D; Tables S4, S5, S6, and S7). For instance, primary *MIR158A* was only found in a NAD<sup>+</sup>-capped form in Col-0 seedlings when they were treated with 0.5 μM ABA, while this RNA was significantly (adjusted p value < 0.01) more NAD<sup>+</sup>-capped in *dxo1* seedlings with and without ABA treatment as compared with Col-0 (Figure S5D; Tables S4, S5, S6, and S7). A similar pattern was noted for primary *MIR398C*, with the only difference being that this *MIRNA* was only NAD<sup>+</sup>-capped in Col-0 seedlings when they were not treated with ABA (Figure S5D; Tables S4, S5, S6, and S7). These findings suggest a potential link between this non-canonical cap modification and miRNA processing.

To investigate the magnitude by which ABA response remodels the landscape of plant transcriptome NAD<sup>+</sup> capping, we directly compared the NAD<sup>+</sup>-capped proportion ( $\log_2[\text{RPM}_{\text{NAD-seq}}/\text{RPM}_{\text{RNA-seq}}]$ ) values for the entire Col-0 and *dxo1* transcriptomes before and during ABA treatment. Using this metric, we found that transcripts with NAD<sup>+</sup> caps were significantly (p value < 0.001, Mann-Whitney *U* test) more abundant in *dxo1* mutant seedlings relative to Col-0 both with and without ABA treatment (Figure 4E), consistent with our original results in unopened flower buds (Figure S2F). These results also revealed that DXO1 regulates numerous NAD<sup>+</sup>-capped transcripts in the Arabidopsis seedling transcriptome with and without ABA treatment (Figures 4D and 4E). Specifically, we found that the overall levels of NAD<sup>+</sup>-capped transcripts were significantly (p value < 0.001, Mann-Whitney *U* test) decreased in both genotypes when they were treated with ABA compared with not treated (Figure 4E), indicating a global loss in NAD<sup>+</sup> capping during ABA treatment. In fact, this analysis revealed that the levels of overall NAD<sup>+</sup> capping in *dxo1* mutant seedlings during ABA response were reduced to levels similar to those identified in Col-0 prior to ABA treatment (Figure 4E; compare the dark blue box to the light orange box). These results indicate that the plant ABA response directs a global decrease of NAD<sup>+</sup> capping in the plant transcriptome that is mostly DXO1-independent.

### The Stability of Transcripts Encoding Master Regulators of ABA Response Is Dynamically Regulated by NAD<sup>+</sup> Capping upon ABA Treatment

To determine the biological functionality of proteins encoded by the NAD<sup>+</sup>-capped mRNAs that dynamically respond to ABA, we

performed GO term analysis. We found that NAD<sup>+</sup>-capped transcripts in both conditions and genotypes were enriched for those encoding proteins involved in ribosome biogenesis, response to cold, and response to salt (Figure 5A), revealing that these classes of transcripts are consistently NAD<sup>+</sup> capped in 12-day-old seedlings. Our results also showed that mRNAs encoding proteins involved in plant response to ABA were modified with a 5' NAD<sup>+</sup> cap in both Col-0 and *dxo1* mutant seedlings in the absence of ABA treatment (Figure 5A), possibly to destabilize these transcripts in the absence of this hormone. Conversely, when seedlings of these same genotypes were treated with ABA, the majority of the population of ABA response protein encoding transcripts lost their 5' NAD<sup>+</sup> caps (Figure 5A), demonstrating that this modification can be potentially used as a dynamic transcriptome addition to regulate specific transcript sets to affect eukaryotic physiological responses.

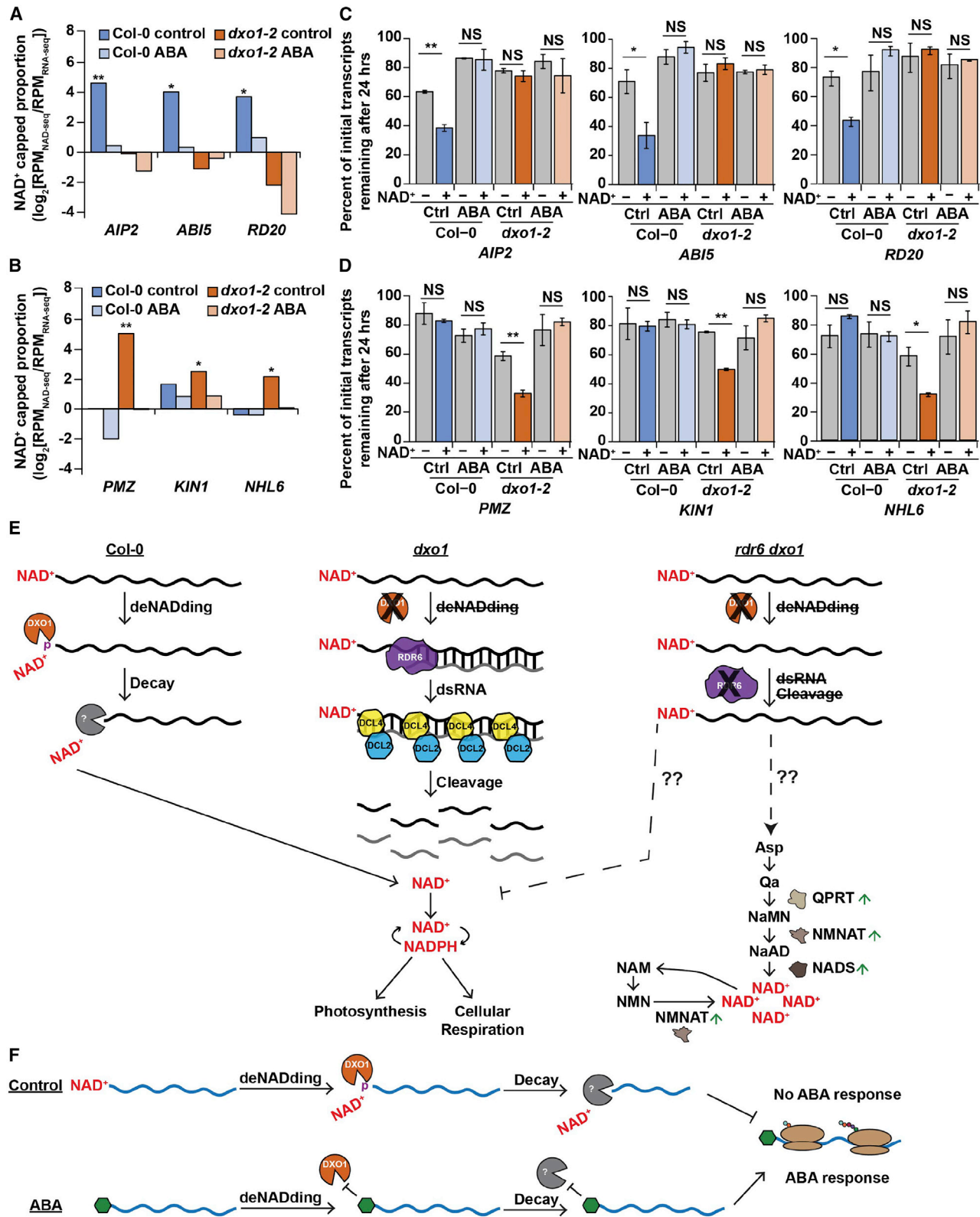
To test the idea that NAD<sup>+</sup> caps can act as dynamic regulators of mRNA stability, we performed GMUCT in both Col-0 and *dxo1* mutant 12-day-old seedlings under control and ABA conditions. The GMUCT libraries were sequenced and provided ~7–18 million mapped reads, and the biological replicates from the distinct genotypes and treatments clustered together (Figure S5E), indicating the high quality and reproducibility of these libraries. Using the proportion uncapped metric, we found that overall the RNAs with high NAD<sup>+</sup>-capped proportion values tended to be significantly (p values < 0.001, Mann-Whitney *U* test) more unstable in all these samples (Figure 5D). In fact, when these collections of NAD<sup>+</sup>-capped transcripts were separated into quartiles based on their increasing NAD<sup>+</sup>-capped proportion ( $\log_2[\text{RPM}_{\text{NAD-seq}}/\text{RPM}_{\text{RNA-seq}}]$ ) values (quartile 1 lowest and 4 highest), we observed significant (all p values < 0.05, Mann-Whitney *U* test) monotonic increases in their proportion uncapped values in both Col-0 and *dxo1-2* mutant seedlings (Figure 5D). Thus, the levels of transcript stability from the identified NAD<sup>+</sup>-capped transcripts decreased as a function of the levels of the total transcript pool identified with a NAD<sup>+</sup> cap for each given mRNA.

We then calculated proportion uncapped fold change ( $\log_2[\text{ABA}/\text{control}]$ ) for each genotype and examined this metric for transcripts that gain, lose, or maintain (common) their NAD<sup>+</sup> capping status in these two genotypes in the context of ABA response (Figures 5E and 5F). We found that 802 and 1,084 mRNAs significantly decreased (lost) and 841 and 612 mRNAs that significantly increased (gained) proportion NAD<sup>+</sup> capping during ABA response in Col-0 and *dxo1* plants, respectively (Figures 5B and 5C). We compared these collections of transcripts to those transcripts that maintained NAD<sup>+</sup> capping in both conditions (341 in Col-0 and 412 in *dxo1* (common)). From this analysis, we found that in both Col-0 and *dxo1* mutant seedlings, transcripts that lost NAD<sup>+</sup> caps during ABA treatment had significantly (p value < 0.001, Mann-Whitney *U* test)

(B and C) The overlap of NAD<sup>+</sup>-capped RNAs identified in 12-day-old Col-0 seedlings (B) and *dxo1-2* seedlings (C) without (dark circle) and with 0.5 μM ABA (light circle) treatment.

(D) The proportion uncapped values for four quartiles of NAD<sup>+</sup>-capped transcripts based on increasing levels of NAD<sup>+</sup>-capped proportion values, with quartile 1 having the lowest values and 4 having the highest in Col-0 and *dxo1-2* mutant seedlings without and with ABA treatment. \*, \*\*, and \*\*\* denote p value < 0.05, 0.01, and 0.001, respectively, Mann-Whitney *U* test.

(E and F) The proportion uncapped fold change ( $\log_2[\text{ABA}/\text{control}]$ ) values for transcripts that lose NAD<sup>+</sup> capping (Left), maintain their NAD<sup>+</sup> capping (Middle), or gain NAD<sup>+</sup> capping (Right) in Col-0 (E) and *dxo1-2* (F) seedlings during ABA treatment as compared with before. \*\*\* denotes p value < 0.001, Mann-Whitney *U* test.



(legend on next page)

test) lower proportion uncapped (more stable) than those transcripts that maintained this moiety in both conditions (Figures 5D and 5E), revealing that transcripts that no longer had a NAD<sup>+</sup> cap during ABA response were stabilized in this process in Col-0 and *dxo1-2* plants. Conversely, transcripts that gained a NAD<sup>+</sup> cap during ABA response demonstrated the exact opposite pattern and were destabilized during ABA treatment in both Col-0 and *dxo1-2* plants (Figures 5D and 5E). These results reveal that the NAD<sup>+</sup> cap modification can be used as a dynamic transcriptome addition to decrease the stability of specific sets of transcripts during eukaryotic physiological responses.

Finally, we looked specifically at the subset of NAD<sup>+</sup>-capped transcripts that are known to be required for plant ABA response (response to ABA GO term) (Figure 5A). We found that 13 of these mRNAs were significantly (*p* value < 0.05, edgeR) NAD<sup>+</sup> capped in Col-0 without ABA treatment (Figures 6A and S6A), and this modification was reduced or lost when these plants were treated with ABA. These 13 mRNAs displayed a reduced level or completely lost NAD<sup>+</sup> capping in *dxo1* mutant seedlings during both conditions (Figures 6A and S6A), thus in the absence of DXO1 function these mRNAs did not demonstrate dynamic NAD<sup>+</sup> capping as occurred in Col-0 plants during ABA response. We also identified 15 other mRNAs encoding ABA response proteins that displayed this dynamic pattern of NAD<sup>+</sup> capping in *dxo1* mutant seedlings, which was mostly absent in Col-0 seedlings (Figures 6B and S6B). In fact, all 28 of these mRNAs encoding ABA response proteins displayed reduced or absent NAD<sup>+</sup> capping during ABA treatment in both genotypes (Figures 6A, 6B, S6A, and S6B).

Our proportion uncapped analyses suggest that ABA-directed NAD<sup>+</sup> capping can dynamically regulate mRNA stability (Figures 5D and 5E). Thus, the mRNAs encoding ABA response proteins that showed a loss of NAD<sup>+</sup> capping in response to ABA treatment in Col-0 and *dxo1* mutant seedlings should display decreased stability when the NAD<sup>+</sup> cap was present and vice versa. To further test this, we treated Col-0 and *dxo1* seedlings with the transcription inhibitors cordycepin and actinomycin D for 0 and 24 h before and during ABA response. We then tested the stability of three transcripts that demonstrate a dynamic decrease in NAD<sup>+</sup> capping in response to ABA in Col-0 (*ABI5* (AT2G36270), *AIP2* (AT5G20910), and *RD20* (AT2G33380)) (Figures 6A and 6C) or in *dxo1* (*PMZ* (AT3G28210), *KIN1*

(AT5G15960), and *NHL6* (AT1G65690)) (Figures 6B and 6D) seedlings by calculating the percentage of initial transcripts remaining 24 h after treatment using RT-qPCR. As expected, we found that significantly (*p* value < 0.05, Student's *t* test) less transcript remained 24 h after transcription inhibition before as compared with after ABA treatment in Col-0 for *ABI5*, *AIP2*, and *RD20* (Figure S6C), as well as in *dxo1* mutant seedlings for *PMZ*, *KIN1*, and *NHL6* (Figure S6D). These findings revealed that the stability of these total transcript pools was significantly lower in the absence of treatment with this phytohormone when their NAD<sup>+</sup> capping levels were significantly higher (Figures 6A and 6B). We also wanted to validate specifically that it was the NAD<sup>+</sup>-capped portion of the transcript population that was destabilized for these specific transcripts (Figure 5D). To do this, we performed NAD<sup>+</sup> capture to distinguish NAD<sup>+</sup>-capped transcripts from the other portion of transcripts for these same six mRNAs following the same treatments with the transcription inhibitors for 0 and 24 h in samples without and with ABA treatment. We found that the levels of NAD<sup>+</sup>-capped transcripts were significantly (*p* value < 0.05, Student's *t* test) lower 24 h after transcription inhibitor treatment as compared with the other portions of these mRNAs in Col-0 without ABA treatment for *ABI5*, *AIP2*, and *RD20* (Figure 6C), as well as in *dxo1* mutant seedlings without ABA treatment for *PMZ*, *KIN1*, and *NHL6* (Figure 6D). Thus, the NAD<sup>+</sup>-capped portion of these transcripts specifically displayed significantly decreased stability in the absence of ABA treatment when their overall levels are lower (Figures 6A and 6B). Ultimately, these findings reveal a previously uncharacterized and essential role of mRNA NAD<sup>+</sup> capping in dynamically regulating the stability of transcripts encoding specific regulators to allow proper ABA response.

## DISCUSSION

### The NAD<sup>+</sup>-Capped Transcriptome Is Controlled in a Developmental-Dependent Manner

We used NAD-seq to study the NAD<sup>+</sup>-capped portion of the Arabidopsis unopened flower bud and 12-day-old seedling with and without ABA treatment transcriptomes for both Col-0 and *dxo1* mutant plants. This analysis revealed that NAD<sup>+</sup>-capped RNAs accumulated in the absence (*dxo1* mutant) as compared with the presence (Col-0) of DXO1 function (Figures 1A, 1B, 4B, and

### Figure 6. Transcripts Encoding Master Regulators of ABA Response Have Their Stability Dynamically Regulated by NAD<sup>+</sup> Capping upon ABA Treatment

(A and B) NAD<sup>+</sup>-capped proportion in Col-0 (blue bars) and *dxo1-2* (orange bars) in the absence (darker colors) or presence (lighter colors) of ABA for ABA-responsive mRNAs that specifically contain a NAD<sup>+</sup> cap in Col-0 (A) or *dxo1-2* (B). \* and \*\* denote *p* value < 0.05 and 0.01, respectively, negative binomial generalized linear model.

(C and D) Percent of total *ABI5*, *AIP2*, and *RD20* (C) and *PMZ*, *KIN1*, and *NHL6* (D) without (–) and with (+) NAD<sup>+</sup> caps remaining 24 h post treatment with transcription inhibitors in Col-0 and *dxo1-2* mutant seedlings without and with ABA treatment. NS denotes no significance. \* and \*\* denote *p* value < 0.05 and 0.01, respectively, Student's *t* test. Error bars indicate ± standard error of the mean.

(E) A model illustrating the link among DXO1-mediated deNADding, small RNA biosynthesis, and NAD<sup>+</sup> biosynthesis. (Left) In Col-0 plants, the NAD<sup>+</sup>-capped transcripts are deNADed by DXO1, releasing the NAD<sup>+</sup> into the free NAD<sup>+</sup> pool. (Middle) In *dxo1* mutant plants, NAD<sup>+</sup>-capped transcripts cannot be deNADed by DXO1, and thus, are subject to RDR6-dependent PTGS, which releases the NAD<sup>+</sup> cap into the free NAD<sup>+</sup> pool. (Right) In *rdr6 dxo1* double mutant plants, the NAD<sup>+</sup> transcripts cannot be deNADed by DXO1 or turned into smRNAs by RDR6-mediated PTGS. Thus, the NAD<sup>+</sup> cap is likely not permitted re-entry to the NAD<sup>+</sup> pool, which may trigger an unknown feedback regulatory mechanism to increase abundance of the mRNAs encoding the NAD<sup>+</sup> biosynthetic enzymes, including *QPRT*, *NMNAT*, and *NADS*, ultimately resulting in the increase of total free NAD<sup>+</sup>.

(F) A model illustrating the dynamic NAD<sup>+</sup> capping changes in the transcriptome before and during ABA response. During normal conditions, the ABA-responsive transcripts (blue) are marked by NAD<sup>+</sup> caps, which are deNADed by DXO1 and are subsequently degraded, resulting in no ABA response. During ABA treatment, ABA-responsive transcripts lack the NAD<sup>+</sup> cap (likely resulting in inclusion of the canonical m<sup>7</sup>G cap instead), which increases their stability and permits proper plant response to ABA.

4D), indicating that DXO1 acts *in vivo* as a deNADding enzyme for the plant transcriptome. Among the DXO1 deNADding substrates identified in Arabidopsis were snoRNAs (Figures 1D and 4D), which is consistent with the findings in human cells (Jiao et al., 2017). In fact, we found that DXO1 deNADded a number of snoRNAs in a tissue-specific manner (Figures 1D and 4D), suggesting this 5' end modification may play a developmental or tissue-specific regulatory function on this class of non-coding RNAs in plant. This idea was also supported by the minimal overlap in the NAD<sup>+</sup>-capped mRNAs identified in Arabidopsis unopened flower buds as compared with 12-day-old seedlings (Figure 4C).

One of the DXO1 deNADding substrates that had not been previously observed in other systems, were several primary MIRNA transcripts, including *MIR158A*, *MIR167A*, *MIR167D*, and *MIR169J*, which were not identified in unopened flower buds but specifically in 12-day-old seedlings that had or had not been treated with 0.5  $\mu$ M ABA (Figures 4D and S5D; Tables S4, S5, S6, and S7), while *MIR398C* was the only one detected in both tissues (Figure 1D; Tables S4, S5, S6, and S7). Recent studies have linked a different reversible covalent RNA modification (N<sup>6</sup>-methyladenosine (m<sup>6</sup>A)) to primary miRNA processing (Alarcón et al., 2015; Bhat et al., 2020), suggesting that future experiments should explore a role for 5' end NAD<sup>+</sup> capping in miRNA processing. In total, our findings revealed that 5' end NAD<sup>+</sup> capping regulates specific subsets of the transcriptome in a tissue-specific manner and may be an important regulatory mechanism throughout development.

### RDR6-Dependent PTGS Processes NAD<sup>+</sup>-Capped Transcripts into smRNAs in the Absence of DXO1

In human cells, NAD<sup>+</sup>-capped mRNAs tend to be more abundant when the function of DXO1 is absent (Jiao et al., 2017). However, our RNA-seq analyses in both plant tissues found that NAD<sup>+</sup>-capped mRNAs were not present at significantly different levels in the absence (*dxo1* mutant) as compared with the presence (Col-0) of DXO1 function (Figures 2A and 2B). Relatedly, we found that NAD<sup>+</sup>-capped RNAs were less stable in Arabidopsis both with and without functionally active DXO1 (both Col-0 and *dxo1* mutant plants, respectively) (Figures 2C, 5D, and 5E). Thus, it is clear that 5' end NAD<sup>+</sup> capping is also a destabilizing mark in plant transcriptomes, but it was unclear what pathway was driving the instability of these transcripts in the absence of DXO1 (*dxo1* mutants). Two recent studies had found that in *dxo1* mutant plants a large collection of mRNAs (> 1,000) were processed into RDR6-dependent smRNAs (Kwasnik et al., 2019; Pan et al., 2020), and we observed the same phenomenon (Figures 3A–3C and S4B–S4D). In fact, we found that this pathway for smRNA processing was producing smRNAs from NAD<sup>+</sup>-capped mRNAs, likely acting as an alternative degradation pathway (Figure 6E). These findings have revealed the intriguing observation that RDR-mediated smRNA processing can be utilized as a bona fide mechanism for breaking down mRNAs containing non-canonical 5' caps and opened up an area of future research inquiry.

The existence of a potential backup mechanism for breaking down 5' NAD<sup>+</sup>-capped mRNAs through smRNA processing, suggested that reacquiring the 5' end NAD<sup>+</sup> from these modified mRNAs is an important physiological process. It also led to the question of how plants respond if both of these degradation mechanisms are missing. Therefore, we determined the overall

NAD<sup>+</sup> levels in Col-0, *dxo1* single, and *rdr6 dxo1* double mutants, and found that overall NAD<sup>+</sup> levels were increased only when both pathways for NAD<sup>+</sup>-capped RNA destabilization were lost (Figure 3D). These results suggested the existence of a feedback pathway for sensing available NAD<sup>+</sup> molecules, and our observation that the transcripts encoding three proteins required for downstream steps of NAD<sup>+</sup> biosynthesis are significantly more abundant in plants that lack both RDR6 and DXO1 (*rdr6 dxo1* double mutants) compared with when one or both are functional (Figures 3E and 3F) also provides initial support for this hypothesis. Future research efforts will be required to identify and characterize the components and mechanisms involved in such a NAD<sup>+</sup> cap sensing and feedback pathway (Figure 6E).

### NAD<sup>+</sup> Capping Is a Dynamic Epitranscriptome Mark Tagging Specific Transcripts for Degradation during Plant ABA Response

The NAD-seq analysis in unopened flower buds showed that a subset of DXO1 deNADding targets encoded proteins required for proper ABA response (Figure 1E), suggesting that this deNADding enzyme functions in ABA regulation of seed germination. We tested this hypothesis and found that indeed DXO1 is required for proper ABA response (Figures 4A and S5A). This phenotype was not a byproduct of the RDR6-dependent smRNAs produced from NAD<sup>+</sup>-capped mRNAs in the absence of DXO1 function (Figure 4B), suggesting that 5' end NAD<sup>+</sup> capping was required for proper ABA response in plants. Our NAD-seq in Col-0 and *dxo1* mutant seedlings with and without ABA treatment revealed that the overall levels of NAD<sup>+</sup> capping decreased in both genotypes (Figure 4E), but especially in *dxo1* mutant seedlings where the number of total genes producing NAD<sup>+</sup>-capped RNAs decreased (Figure 4D). Thus, ABA treatment results in significant and dynamic changes to the NAD<sup>+</sup>-capped transcriptome in plants, revealing that this, like other RNA modifications (e.g., m<sup>6</sup>A) (Anderson et al., 2018; Nachtergaele and He, 2017), can be added and removed from specific RNAs in response to specific physiological conditions.

A major collection of mRNAs that displayed a significant decrease in NAD<sup>+</sup> capping levels in both Col-0 and *dxo1* mutant seedlings were those encoding regulators of ABA response (Figures 5A, 6A, 6B, S6A, and S6B). Given that NAD<sup>+</sup> capping is a destabilizing mark when present on Arabidopsis mRNAs (Figures 2C, 5D, 5E, 6C, 6D, S6C, and S6D), we reasoned that the dynamic loss of NAD<sup>+</sup> caps would result in the stabilization of these transcripts in response ABA treatment. As expected, we found that the dynamic loss of NAD<sup>+</sup> caps during ABA response significantly increased stability of the corresponding transcripts and vice versa (Figures 5D, 5E, 6C, 6D, S6C, and S6D). Relatedly, a collection of 28 transcripts encoding ABA response proteins displayed interesting patterns of NAD<sup>+</sup> capping dynamics in response to ABA treatment in the absence of DXO1 function (in *dxo1* mutant seedlings) (Figures 6A, 6B, S6A, and S6B). This overall improper regulation of such a large collection of mRNAs encoding ABA response proteins provides a compelling explanation for the ABA hyposensitivity of *dxo1* mutant plants (Figures 4A, 4B, and S5A). Furthermore, the decrease in 5' NAD<sup>+</sup> capping of these 28 mRNAs in *dxo1* mutant plants (Figures 6A, 6B, S6A, and S6B) reveals that this dynamic response does not require the functionality of DXO1. Thus, the dynamic regulation of 5' end

NAD<sup>+</sup> capping during ABA response could be directed by another enzyme(s) with deNADding activity, which are prevalent in the Arabidopsis genome (Yoshimura and Shigeoka, 2015), or by the machinery responsible for adding this epitranscriptome mark in eukaryotic transcriptomes, with neither of these models being mutually exclusive. In conclusion, our study reveals that plant ABA response remodels the NAD<sup>+</sup>-capped transcriptome even in the absence of DXO1 function (Figure 6F), thus providing evidence that mRNA NAD<sup>+</sup> caps can be dynamically regulated to affect a eukaryotic physiological response.

## STAR★METHODS

Detailed methods are provided in the online version of this paper and include the following:

- KEY RESOURCES TABLE
- RESOURCE AVAILABILITY
  - Lead Contact
  - Materials Availability
  - Data and Code Availability
- EXPERIMENTAL MODEL AND SUBJECT DETAILS
  - Plant Materials
  - Generation of pDXO1::DXO1-GUS::DXO1-3'UTR dxo1-2 Plants
  - Generation of pUBQ10::DXO1-eGFP dxo1-2 Plants
- METHOD DETAILS
  - Histochemical Analysis of pDXO1::DXO1-GUS dxo1-2 Plants
  - DXO1 Subcellular Localization Analysis Using pUBQ10::DXO1-eGFP/dxo1-2 Plants
  - Validation of NAD<sup>+</sup> Capture Approach Using *In Vitro* Luciferase Transcription
  - RNA Extraction
  - *In Vivo* NAD-seq Library Construction
  - Validation of NAD-seq by NAD-qPCR
  - polyA-selected and Total RNA-seq (mRNA- and RNA-seq) Library Construction
  - smRNA-seq Library Construction
  - Genome-wide Mapping of Uncapped and Cleaved Transcripts (GMUCT)
  - Germination Test during ABA Treatment
  - Liquid Chromatography-High Resolution Mass Spectrometry (LC-HRMS) to Detect Total NAD<sup>+</sup>
  - qRT-PCR to Detect NAD<sup>+</sup> Biosynthesis Genes
  - Transcript Stability Time Course
- QUANTIFICATION AND STATISTICAL ANALYSIS
  - Identification of NAD<sup>+</sup> Capped RNAs
  - Measurement of mRNA Stability Using the Proportion Uncapped Metric
  - Differential Abundance Analysis
  - Small RNA Profiling
  - Determination of Library Reproducibility
  - Construction of a DXO1 Phylogenetic Tree

## SUPPLEMENTAL INFORMATION

Supplemental Information can be found online at <https://doi.org/10.1016/j.devcel.2020.11.009>.

## ACKNOWLEDGMENTS

The authors would like to thank members of the B.D.G. lab, both past and present for helpful discussions. This work was funded by NSF, United States grants IOS-2023310 and IOS-1849708 to B.D.G. and R01GM132261 to N.W.S.; S.T. is supported by the American Diabetes Association, United States through post-doctoral fellowship 1-19-PDF-144. The funders had no role in study design, data collection and analysis, decision to publish, or preparation of the manuscript.

## AUTHOR CONTRIBUTIONS

B.D.G. conceived the study. X.Y., M.R.W., S.T., N.W.S., and B.D.G. designed the experiments. X.Y., M.R.W., L.E.V., S.T., J.S., R.G., N.W.S., and B.D.G. performed experiments. X.Y., S.T., M.C.K., N.W.S., E.L., and B.D.G. analyzed the data. X.Y., M.C.K., and B.D.G. wrote the paper with assistance from all authors. The authors have read and approved the manuscript for publication.

## DECLARATION OF INTERESTS

The authors declare no competing interests.

Received: May 20, 2020

Revised: September 2, 2020

Accepted: November 6, 2020

Published: December 7, 2020

## REFERENCES

- Alarcón, C.R., Lee, H., Goodarzi, H., Halberg, N., and Tavazoie, S.F. (2015). N6-methyladenosine marks primary microRNAs for processing. *Nature* 519, 482–485.
- Anders, S., Pyl, P.T., and Huber, W. (2015). HTSeq—a Python framework to work with high-throughput sequencing data. *Bioinformatics* 31, 166–169.
- Anderson, S.J., Kramer, M.C., Gosai, S.J., Yu, X., Vandivier, L.E., Nelson, A.D.L., Anderson, Z.D., Beilstein, M.A., Fray, R.G., Lyons, E., and Gregory, B.D. (2018). N6-methyladenosine inhibits local ribonucleolytic cleavage to stabilize mRNAs in Arabidopsis. *Cell Rep.* 25, 1146–1157.e3.
- Baulcombe, D.C. (1996). Mechanisms of pathogen-derived resistance to viruses in transgenic plants. *Plant Cell* 8, 1833–1844.
- Bhat, S.S., Bielewicz, D., Gulanicz, T., Bodi, Z., Yu, X., Anderson, S.J., Szewc, L., Bajczyk, M., Dolata, J., Grzelak, N., et al. (2020). mRNA adenosine methylase (MTA) deposits m<sup>6</sup>A on pri-miRNAs to modulate miRNA biogenesis in *Arabidopsis thaliana*. *Proc. Natl. Acad. Sci. USA* 117, 21785–21795.
- Bird, J.G., Basu, U., Kuster, D., Ramachandran, A., Grudzien-Nogalska, E., Towheed, A., Wallace, D.C., Kiledjian, M., Temiakov, D., Patel, S.S., et al. (2018). Highly efficient 5' capping of mitochondrial RNA with NAD<sup>+</sup> and NADH by yeast and human mitochondrial RNA polymerase. *eLife* 7, e42179.
- Bird, J.G., Zhang, Y., Tian, Y., Panova, N., Barvík, I., Greene, L., Liu, M., Buckley, B., Krásný, L., Lee, J.K., et al. (2016). The mechanism of RNA 5' capping with NAD<sup>+</sup>, NADH and desphospho-CoA. *Nature* 535, 444–447.
- Cahová, H., Winz, M.L., Höfer, K., Nübel, G., and Jäschke, A. (2015). NAD captureSeq indicates NAD as a bacterial cap for a subset of regulatory RNAs. *Nature* 519, 374–377.
- Chang, J.H., Jiao, X., Chiba, K., Oh, C., Martin, C.E., Kiledjian, M., and Tong, L. (2012). Dxo1 is a new type of eukaryotic enzyme with both decapping and 5'-3' exoribonuclease activity. *Nat. Struct. Mol. Biol.* 19, 1011–1017.
- Chen, Y.G., Kowtoniuk, W.E., Agarwal, I., Shen, Y., and Liu, D.R. (2009). LC/MS analysis of cellular RNA reveals NAD-linked RNA. *Nat. Chem. Biol.* 5, 879–881.
- Chiu, W., Niwa, Y., Zeng, W., Hirano, T., Kobayashi, H., and Sheen, J. (1996). Engineered GFP as a vital reporter in plants. *Curr. Biol.* 6, 325–330.
- Dobin, A., Davis, C.A., Schlesinger, F., Drenkow, J., Zaleski, C., Jha, S., Batut, P., Chaisson, M., and Gingeras, T.R. (2013). STAR: ultrafast universal RNA-seq aligner. *Bioinformatics* 29, 15–21.

- Donnelly, P.M., Bonetta, D., Tsukaya, H., Dengler, R.E., and Dengler, N.G. (1999). Cell cycling and cell enlargement in developing leaves of Arabidopsis. *Dev. Biol.* *215*, 407–419.
- Finkelstein, R. (2013). Abscisic acid synthesis and response. *Arabidopsis Book* *11*, e0166.
- Frederick, D.W., Trefely, S., Buas, A., Goodspeed, J., Singh, J., Mesaros, C., Baur, J.A., and Snyder, N.W. (2017). Stable isotope labeling by essential nutrients in cell culture (SILEC) for accurate measurement of nicotinamide adenine dinucleotide metabolism. *Analyst* *142*, 4431–4437.
- Frindert, J., Zhang, Y., Nübel, G., Kahloon, M., Kolmar, L., Hotz-Wagenblatt, A., Burhenne, J., Haefeli, W.E., and Jäschke, A. (2018). Identification, biosynthesis, and decapping of NAD-capped RNAs in *B. subtilis*. *Cell Rep.* *24*, 1890–1901.e8.
- Gonatopoulos-Pournatzis, T., and Cowling, V.H. (2014). Cap-binding complex (CBC). *Biochem. J.* *457*, 231–242.
- Gosai, S.J., Foley, S.W., Wang, D., Silverman, I.M., Selamoglu, N., Nelson, A.D.L., Beilstein, M.A., Daldal, F., Deal, R.B., and Gregory, B.D. (2015). Global analysis of the RNA-protein interaction and RNA secondary structure landscapes of the Arabidopsis nucleus. *Mol. Cell* *57*, 376–388.
- Gregory, B.D., O'Malley, R.C., Lister, R., Ulrich, M.A., Tonti-Filippini, J., Chen, H., Millar, A.H., and Ecker, J.R. (2008). A link between RNA metabolism and silencing affecting Arabidopsis development. *Dev. Cell* *14*, 854–866.
- Hashida, S.N., Takahashi, H., and Uchimiya, H. (2009). The role of NAD biosynthesis in plant development and stress responses. *Ann. Bot.* *103*, 819–824.
- Herr, A.J., Molnár, A., Jones, A., and Baulcombe, D.C. (2006). Defective RNA processing enhances RNA silencing and influences flowering of Arabidopsis. *Proc. Natl. Acad. Sci. USA* *103*, 14994–15001.
- Huang, da W., Sherman, B.T., and Lempicki, R.A. (2009). Systematic and integrative analysis of large gene lists using DAVID bioinformatics resources. *Nat. Protoc.* *4*, 44–57.
- Hugouvieux, V., Kwak, J.M., and Schroeder, J.I. (2001). An mRNA cap binding protein, ABH1, modulates early abscisic acid signal transduction in Arabidopsis. *Cell* *106*, 477–487.
- Jiao, X., Doamekpor, S.K., Bird, J.G., Nickels, B.E., Tong, L., Hart, R.P., and Kiledjian, M. (2017). 5' End nicotinamide adenine dinucleotide Cap in human cells promotes RNA decay through DXO-Mediated deNADding. *Cell* *168*, 1015–1027.e10.
- Kiledjian, M. (2018). Eukaryotic RNA 5'-end NAD + capping and DeNADding. *Trends Cell Biol.* *28*, 454–464.
- Klepikova, A.V., Kasianov, A.S., Gerasimov, E.S., Logacheva, M.D., and Penin, A.A. (2016). A high resolution map of the Arabidopsis thaliana developmental transcriptome based on RNA-seq profiling. *Plant J.* *88*, 1058–1070.
- Kwasnik, A., Wang, V.Y.-F., Krzysztos, M., Gozdek, A., Zakrzewska-Placzek, M., Stepniak, K., Poznanski, J., Tong, L., and Kufel, J. (2019). Arabidopsis DXO1 links RNA turnover and chloroplast function independently of its enzymatic activity. *Nucleic Acids Res.* *47*, 4751–4764.
- Li, F., Zheng, Q., Ryykin, P., Dragomir, I., Desai, Y., Aiyer, S., Valladares, O., Yang, J., Bambina, S., Sabin, L.R., et al. (2012). Global analysis of RNA secondary structure in two metazoans. *Cell Rep.* *1*, 69–82.
- Liu, L., and Chen, X. (2016). RNA quality control as a key to suppressing RNA silencing of endogenous genes in plants. *Mol. Plant* *9*, 826–836.
- Love, M.I., Huber, W., and Anders, S. (2014). Moderated estimation of fold change and dispersion for RNA-seq data with DESeq2. *Genome Biol.* *15*, 550.
- Lyons, E., Pedersen, B., Kane, J., Alam, M., Ming, R., Tang, H., Wang, X., Bowers, J., Paterson, A., Lisch, D., and Freeling, M. (2008). Finding and comparing syntenic regions among Arabidopsis and the outgroups papaya, poplar, and grape: CoGe with Rosids. *Plant Physiol.* *148*, 1772–1781.
- Martin, M. (2011). Cutadapt removes adapter sequences from high-throughput sequencing reads. *EMBnet J.* *17*, 10.
- Martínez de Alba, A.E., Moreno, A.B., Gabriel, M., Mallory, A.C., Christ, A., Bounon, R., Balzergue, S., Aubourg, S., Gautheret, D., Crespi, M.D., et al. (2015). In plants, decapping prevents RDR6-dependent production of small interfering RNAs from endogenous mRNAs. *Nucleic Acids Res.* *43*, 2902–2913.
- Nachtergaele, S., and He, C. (2017). The emerging biology of RNA post-transcriptional modifications. *RNA Biol.* *14*, 156–163.
- Pan, S., Li, K.E., Huang, W., Zhong, H., Wu, H., Wang, Y., Zhang, H., Cai, Z., Guo, H., Chen, X., and Xia, Y. (2020). Arabidopsis DXO1 possesses deNADding and exonuclease activities and its mutation affects defense-related and photosynthetic gene expression. *J. Integr. Plant. Biol.* *62*, 967–983.
- Peragine, A., Yoshikawa, M., Wu, G., Albrecht, H.L., and Poethig, R.S. (2004). SGS3 and SGS2/SDE1/RDR6 are required for juvenile development and the production of trans-acting siRNAs in Arabidopsis. *Genes Dev.* *18*, 2368–2379.
- Robinson, M.D., McCarthy, D.J., and Smyth, G.K. (2010). edgeR: a Bioconductor package for differential expression analysis of digital gene expression data. *Bioinformatics* *26*, 139–140.
- Silverman, I.M., Li, F., Alexander, A., Goff, L., Trapnell, C., Rinn, J.L., and Gregory, B.D. (2014). RNase-mediated protein footprint sequencing reveals protein-binding sites throughout the human transcriptome. *Genome Biol.* *15*, R3.
- Tamura, K., Peterson, D., Peterson, N., Stecher, G., Nei, M., and Kumar, S. (2011). MEGA5: molecular evolutionary genetics analysis using maximum likelihood, evolutionary distance, and maximum parsimony methods. *Mol. Biol. Evol.* *28*, 2731–2739.
- Thimm, O., Bläsing, O., Gibon, Y., Nagel, A., Meyer, S., Krüger, P., Selbig, J., Müller, L.A., Rhee, S.Y., and Stitt, M. (2004). mapman: a user-driven tool to display genomics data sets onto diagrams of metabolic pathways and other biological processes. *Plant J.* *37*, 914–939.
- Valkov, E., Muthukumar, S., Chang, C.T., Jonas, S., Weichenrieder, O., and Izaurralde, E. (2016). Structure of the Dcp2–Dcp1 mRNA-decapping complex in the activated conformation. *Nat. Struct. Mol. Biol.* *23*, 574–579.
- Vandivier, L.E., Campos, R., Kuksa, P.P., Silverman, I.M., Wang, L.S., and Gregory, B.D. (2015). Chemical modifications mark alternatively spliced and uncapped messenger RNAs in Arabidopsis. *Plant Cell* *27*, 3024–3037.
- Vvedenskaya, I.O., Bird, J.G., Zhang, Y., Zhang, Y., Jiao, X., Barvík, I., Krásný, L., Kiledjian, M., Taylor, D.M., Ebright, R.H., and Nickels, B.E. (2018). CapZyme-Seq comprehensively defines promoter-sequence determinants for RNA 5' capping with NAD<sup>+</sup>. *Mol. Cell* *70*, 553–564.e9.
- Walters, R.W., Matheny, T., Mizoue, L.S., Rao, B.S., Muhlrad, D., and Parker, R. (2017). Identification of NAD<sup>+</sup> capped mRNAs in *Saccharomyces cerevisiae*. *Proc. Natl. Acad. Sci. USA* *114*, 480–485.
- Wang, Y., Li, S., Zhao, Y., You, C., Le, B., Gong, Z., Mo, B., Xia, Y., and Chen, X. (2019). NAD<sup>+</sup>-capped RNAs are widespread in the Arabidopsis transcriptome and can probably be translated. *Proc. Natl. Acad. Sci. USA* *116*, 12094–12102.
- Wawer, I., Golisz, A., Sulkowska, A., Kawa, D., Kulik, A., and Kufel, J. (2018). mRNA decapping and 5'-3' decay contribute to the regulation of ABA signaling in Arabidopsis thaliana. *Front. Plant Sci.* *9*, 312.
- Willmann, M.R., Berkowitz, N.D., and Gregory, B.D. (2014). Improved genome-wide mapping of uncapped and cleaved transcripts in eukaryotes—GMUCT 2.0. *Methods* *67*, 64–73.
- Willmann, M.R., Endres, M.W., Cook, R.T., and Gregory, B.D. (2011). The functions of RNA-dependent RNA polymerases in Arabidopsis. *Arabidopsis Book* *9*, e0146.
- Xiang, C., Han, P., Lutziger, I., Wang, K., and Oliver, D.J. (1999). A mini binary vector series for plant transformation. *Plant Mol. Biol.* *40*, 711–717.
- Xiang, S., Cooper-Morgan, A., Jiao, X., Kiledjian, M., Manley, J.L., and Tong, L. (2009). Structure and function of the 5' → 3' exonuclease Rat1 and its activating partner ral1. *Nature* *458*, 784–788.
- Xiao, W., Wang, R.S., Handy, D.E., and Loscalzo, J. (2018). NAD(H) and NADP(H) redox couples and cellular energy metabolism. *Antioxid. Redox Signal.* *28*, 251–272.
- Yoshimura, K., and Shigeoka, S. (2015). Versatile physiological functions of the Nudix hydrolase family in Arabidopsis. *Biosci. Biotechnol. Biochem.* *79*, 354–366.
- Yu, X., Willmann, M.R., Anderson, S.J., and Gregory, B.D. (2016). Genome-wide mapping of uncapped and cleaved transcripts reveals a role for the

nuclear mRNA cap-binding complex in Cotranslational RNA decay in Arabidopsis. *Plant Cell* 28, 2385–2397.

Zhang, H., Zhong, H., Zhang, S., Shao, X., Ni, M., Cai, Z., Chen, X., and Xia, Y. (2019). NAD tagSeq reveals that NAD<sup>+</sup>-capped RNAs are mostly produced from a large number of protein-coding genes in Arabidopsis. *Proc. Natl. Acad. Sci. USA* 116, 12072–12077.

Zhang, X., and Guo, H. (2017). mRNA decay in plants: both quantity and quality matter. *Curr. Opin. Plant Biol.* 35, 138–144.

Zhang, X., Zhu, Y., Liu, X., Hong, X., Xu, Y., Zhu, P., Shen, Y., Wu, H., Ji, Y., Wen, X., et al. (2015). Plant biology. Suppression of endogenous gene silencing by bidirectional cytoplasmic RNA decay in Arabidopsis. *Science* 348, 120–123.

Zheng, Q., Ryzkin, P., Li, F., Dragomir, I., Valladares, O., Yang, J., Cao, K., Wang, L.S., and Gregory, B.D. (2010). Genome-wide double-stranded RNA sequencing reveals the functional significance of base-paired RNAs in Arabidopsis. *PLoS Genet.* 6, e1001141.

**STAR★METHODS**

**KEY RESOURCES TABLE**

REAGENT or RESOURCE	SOURCE	IDENTIFIER
<b>Chemicals, Peptides, and Recombinant Proteins</b>		
Abcisic acid (ABA)	Sigma-Aldrich	Cat#A4906
Na-HEPES	Sigma-Aldrich	Cat#H7006
ADP-ribosylcyclase (ADPRC)	Sigma-Aldrich	Cat#A9106-1VL
4-pentyn-1-ol	Sigma-Aldrich	Cat#302481
β-Nicotinamide adenine dinucleotide hydrate (NAD)	Sigma-Aldrich	Cat#N7004
CuSO <sub>4</sub>	Sigma-Aldrich	Cat#C1297
THPTA	Sigma-Aldrich	Cat#762342
Sodium ascorbate	Sigma-Aldrich	Cat#A7631
Biotin azide	Sigma-Aldrich	Cat#CLK-AZ104P4-25
Acetylated BSA	Sigma-Aldrich	Cat#B8894
X-Gluc (5-bromo-4-chloro-3-indolyl β-D-glucuronide)	Sigma-Aldrich	Cat#B5285
Sucrose	Sigma-Aldrich	Cat#S8501
Dynabeads MyOne Streptavidin C1	Thermo Fisher Sci.	Cat#65001
RNaseOUT	Thermo Fisher Sci.	Cat#LS10777019
T4 polynucleotide kinase	New England Biolabs	Cat#M0201S
T4 RNA ligase 1	New England Biolabs	Cat#M0204S
T4 RNA ligase 2, truncated	New England Biolabs	Cat#M0242S
10× NEB Buffer 2	New England Biolabs	Cat#B7002S
10mM ATP	New England Biolabs	Cat#P0756S
Duplex Specific Nuclease (DSN)	Evrogen	Cat#EA001
50 mM dNTPs (12.5 mM of each)	Promega	Cat#U1420
Sodium Acetate (3 M), pH 5.5, RNase-free	Thermo Fisher Sci.	Cat#AM9740
Glycogen	Thermo Fisher Sci.	Cat#AM9510
Qiazol	Qiagen	Cat#79306
Chloroform:Isoamyl alcohol	Sigma-Aldrich	Cat#C0549
Phenol:chloroform	Sigma-Aldrich	Cat#77617
2-propanol	Sigma-Aldrich	Cat#34863
EDTA	Sigma-Aldrich	Cat#BP2483
100% ethanol	Decon Labs	Cat#2716
Urea	Thermo Fisher Sci.	Cat#BP169
Tris-HCL	Thermo Fisher Sci.	Cat#15567-027
NaCl (5 M), RNase-free	Thermo Fisher Sci.	Cat#AM9759
Magnesium Chloride (MgCl <sub>2</sub> ), 1 M Solution	Affymatrix	Cat#78641
Actinomycin D	Research Products International	Cat#A10025-0.005
Cordycepin	Sigma-Aldrich	Cat#C3394-25MG
<b>Critical Commercial Assays</b>		
TaqI	New England Biolabs	Cat#TaqI-v2
MEGAscript T7 Transcription Kit	Thermo Fisher Sci.	Cat#AM1334
Dynabeads mRNA DIRET Purification Kit	Thermo Fisher Sci.	Cat#61011
miRNeasy Mini Kit	Qiagen	Cat#217004
RNA Fragmentation Reagents	Thermo Fisher Sci.	Cat#AM8740
RNase-Free DNase Set	Qiagen	Cat#79254
SuperScript II Reverse Transcriptase	Thermo Fisher Sci.	Cat#18064014

(Continued on next page)

**Continued**

REAGENT or RESOURCE	SOURCE	IDENTIFIER
Phusion High-Fidelity DNA Polymerase	New England Biolabs	Cat#M0531S
2x SYBR Green qPCR Master Mix	Bimake	Cat#B21202
<b>Deposited Data</b>		
Raw and processed NAD captureSeq (NADseq) data	This paper	GEO: GSE142390
Raw and processed polyA+-selected RNA sequencing (mRNA-seq) data	This paper	GEO: GSE142390
Raw and processed small RNA sequencing (smRNAseq) data	This paper	GEO: GSE142390
Raw and processed GMUCT data	This paper	GEO: GSE142390
Raw and processed GMUCT data (Col-0)	<a href="#">Willmann et al., 2014</a>	GEO: GSE47121
EPIC-CoGe genome browser	<a href="#">Lyons and Freeling, 2008</a>	<a href="https://genomevolution.org/coge/NotebookView.pl?nid=2708">https://genomevolution.org/coge/NotebookView.pl?nid=2708</a>
TAIR10 Arabidopsis annotation	TAIR	<a href="ftp://ftp.arabidopsis.org/home/tair/Genes/TAIR10_genome_release/">ftp://ftp.arabidopsis.org/home/tair/Genes/TAIR10_genome_release/</a>
<b>Experimental Models: Organisms/Strains</b>		
Arabidopsis thaliana: Col-0	ABRC	CS70000
Arabidopsis thaliana: <i>dxo1-1</i>	ABRC	SALK_103157
Arabidopsis thaliana: <i>dxo1-2</i>	ABRC	SALK_032903
Arabidopsis thaliana: <i>rdr6-11</i>	<a href="#">Peragine et al., 2004</a>	CS67869
Arabidopsis thaliana: <i>rdr6-11 dxo1-2</i>	This study	N/A
Arabidopsis thaliana: <i>pDXO1::DXO1-GUS dxo1-2</i>	This study	N/A
Arabidopsis thaliana: <i>pUBQ10::DXO1-eGFP dxo1-2</i>	This study	N/A
<b>Oligonucleotides</b>		
Oligo(dT) <sub>12-18</sub> primers	Thermo Fisher Sci.	Cat#18418012
Genotyping primers	<a href="#">Table S8</a> ; this study	N/A
TruSeq adaptors, primers and indices	Illumina	TruSeq Small RNA Sample Prep Kit
TruSeq RA3 3'-adapter with random hexamer primer	<a href="#">Willmann et al., 2014</a>	N/A
qPCR primers	<a href="#">Table S8</a> ; this study	N/A
<b>Software and Algorithms</b>		
cutadapt v1.9.1	<a href="#">Martin, 2011</a>	<a href="https://cutadapt.readthedocs.io/en/stable/installation.html">https://cutadapt.readthedocs.io/en/stable/installation.html</a>
STAR v2.4.2a	<a href="#">Dobin et al., 2013</a>	<a href="https://github.com/alexdobin/STAR">https://github.com/alexdobin/STAR</a>
HTseq v0.6.0	<a href="#">Anders et al., 2015</a>	<a href="https://github.com/simon-anders/htseq">https://github.com/simon-anders/htseq</a>
DEseq2 v1.18.1	<a href="#">Love et al., 2014</a>	<a href="https://bioconductor.org/biocLite.R">https://bioconductor.org/biocLite.R</a>
edgeR v3.26.6	<a href="#">Robinson et al., 2010</a>	<a href="https://bioconductor.org/biocLite.R">https://bioconductor.org/biocLite.R</a>
DAVID online tool	<a href="#">Huang et al., 2009</a>	<a href="https://david.ncifcrf.gov">https://david.ncifcrf.gov</a>
MEGA v5.2	<a href="#">Tamura et al., 2011</a>	<a href="https://www.megasoftware.net">https://www.megasoftware.net</a>
<b>Other</b>		
MS salts	Phytotech	Cat#M524
Phytoblend	Caisson	Cat#PTP01

**RESOURCE AVAILABILITY**

**Lead Contact**

Further information and requests for resources and reagents should be directed to and will be fulfilled by the Lead Contact, Dr. Brian D. Gregory ([bdgregor@sas.upenn.edu](mailto:bdgregor@sas.upenn.edu)).

**Materials Availability**

All constructs and plant lines developed for this project are available upon request to the Lead Contact, Dr. Brian D. Gregory ([bdgregor@sas.upenn.edu](mailto:bdgregor@sas.upenn.edu)).

### Data and Code Availability

The raw and processed data for NAD-seq, total RNA-seq, GMUCT, polyA-selected (polyA) RNA-seq (mRNA-seq), and smRNA-seq libraries made with RNA extracted from unopened flower buds and 12-day-old seedlings (with and without 0.5  $\mu$ M ABA treatment) of Col-0 and *dxo1* mutants as well as smRNA-seq libraries for *rdp6-11 dxo1-2* unopened flower buds has been deposited in the NCBI Gene Expression Omnibus (<http://www.ncbi.nlm.nih.gov/geo>) database under the accession number GEO: GSE142390. Previously published GMUCT data for Col-0 unopened flower buds were obtained from GEO using the accession number GEO: GSE47121 (Willmann et al., 2014). The gene accession numbers for *DXO1* and *RDR6* are *AT4G17620* and *AT3G49500*, respectively. The sequencing data presented here is also available through the EPIC-CoGe genome browser (Lyons et al., 2008): <https://genomevolution.org/coge/NotebookView.pl?nid=2708>.

## EXPERIMENTAL MODEL AND SUBJECT DETAILS

### Plant Materials

All plant lines used in this study were in the genetic background of *Arabidopsis thaliana* Columbia-0 (Col-0) ecotype. Plants of the Col-0 ecotype served as our wild-type plants in all experiments. Two T-DNA insertion alleles of the *DXO1* gene (*AT4G17620*) in the genetic background of *Arabidopsis thaliana* Columbia-0 (Col-0) ecotype from the Salk Insertional Mutant Collection were used in this study. One is SALK\_103157 (*dxo1-1*) that has a T-DNA insertion in the second exon, and other is SALK\_032903 (*dxo1-2*) which contains a T-DNA insertion in the fifth intron. *dxo1-2* was crossed with *rdp6-11* to obtain the double mutant *rdp6-11 dxo1-2*. The primers used for genotyping these various mutant lines are listed in Table S8. The genotyping for the *rdp6-11* mutation was performed by amplifying DNA samples with the primers listed in Table S8, and digesting the resulting PCR products with Taq1. Samples displaying two bands with lengths of 109 base pairs (bp) and 78 bp are *rdp6-11* homozygotes, samples showing two bands with lengths of 94 bp and 78 bp are wild-type plants, and samples showing all the three bands (109 bp, 94 bp and 78 bp), are heterozygotes (Peragine et al., 2004).

All plants used in this study were grown in growth chambers under long days conditions (16 hours light and 8 hours dark photoperiod) at 22°C. For sampling unopened flower buds as well as phenotypic analyses of all genetic backgrounds, these plants were grown on soil. For sampling and analyzing 12-day-old seedlings with and without ABA treatment, these plants were grown vertically on ½ Murashige and Skoog (MS) medium (Phytotech Labs, Lenexa, KS, USA) without and with varying concentrations of ABA.

### Generation of pDXO1::DXO1-GUS::DXO1-3'UTR *dxo1-2* Plants

*pDXO1::DXO1-GUS::DXO1-3'UTR* was made starting with a modified version of pCAMBIA3301 that had the *p35S::BAR* fragment replaced with *pNOS::BAR* which was amplified from pCB302 (Xiang et al., 1999), restricting the PCR fragment with BstXI and XhoI, and inserting it into pCAMBIA3301. The starting clone also had everything removed between EcoRI and BstEII and replaced with a DNA sequence that included EcoRI, StuI, RsrII, and BstEII sites, in that order. The *DXO1* 3' UTR was amplified from just downstream of the *DXO1* stop codon to just before the start codon of the downstream gene (*AT4G17640*). This 592 bp product was restricted with RsrII and BstEII and inserted between those two sites of the vector. Then, the *DXO1* promoter and coding region were amplified from Col-0 genomic DNA, amplifying from immediately downstream of the upstream gene's (*AT4G17616*) stop codon through the coding region of *AT4G17620* (*DXO1*) but not including the stop codon. The 3236 bp product was restricted to completion by StuI and partially with EcoRI because the 3236 bp product had an internal EcoRI site and was inserted between the EcoRI and StuI sites of the modified pCAMBIA3301 vector. Finally, GUS was amplified from pCAMBIA3301, restricted with StuI and RsrII, and inserted between those sites of the vector. The construct was transformed into *dxo1-2* mutant plants through floral dip. All primers are listed in Table S8.

### Generation of pUBQ10::DXO1-eGFP *dxo1-2* Plants

*pUBQ10::DXO1-eGFP* was made starting with a modified version of pCAMBIA3301 that had the *p35S::BAR* fragment replaced with *pNOS::BAR* which was amplified from pCB302 (Xiang et al., 1999), restricting the PCR fragment with BstXI and XhoI, and inserting it into pCAMBIA3301. A *pUBQ10-SpeI-MCS-NcoI-UBQ10* 3'UTR cassette was restricted from the pSY06 clone with HindIII and EcoRI and inserted between the HindIII and EcoRI sites of the modified version of pCAMBIA3301 vector. The resulting plasmid was then restricted with HindIII and BstEII, blunted, and ligated to remove *p35S::GUS*. The pUBQ10 was 636 bp and the 3'UTR was 382 bp. The *DXO1* CDS (but not including the stop codon) was amplified from cDNA of Col-0, fully restricted with StuI (a site in the MCS) and partially with SpeI, and the 1644 bp product was inserted between the SpeI and StuI sites within the vector. eGFP was amplified from the vector HBT95 (Chiu et al., 1996) with primers specified in Table S8, restricted with StuI and NcoI, and inserted. The construct was transformed into *dxo1-2* mutant plants through floral dip. All primers are listed in Table S8.

## METHOD DETAILS

### Histochemical Analysis of pDXO1::DXO1-GUS *dxo1-2* Plants

For histochemical analysis of *pDXO1::DXO1-GUS dxo1-2* plants, different tissues from multiple developmental stages were collected and stained with 5-bromo-4-chloro-3-indolyl  $\beta$ -D-glucuronide (X-gluc) (Sigma-Aldrich, St. Louis, MO, USA). To do this, the collected tissues were placed in 90% acetone for 15 minutes on ice, and then in X-Gluc buffer under vacuum for 16 hours at room temperature. After that, the samples were viewed via microscopy (Donnelly et al., 1999).

### DXO1 Subcellular Localization Analysis Using *pUBQ10::DXO1-eGFP/dxo1-2* Plants

To determine the subcellular localization of DXO1, Arabidopsis protoplasts and root tips of *T<sub>2</sub>pUBQ10::DXO1-eGFP dxo1-2* plants were analyzed using a fluorescent microscope.

### Validation of NAD<sup>+</sup> Capture Approach Using *In Vitro* Luciferase Transcription

Luciferase transcripts (*LUC*) with NAD<sup>+</sup> modification were *in vitro* transcribed using MEGAScript T7 Transcription Kit (ThermoFisher Scientific, Waltham, MA, USA) with the addition of the non-canonical nucleotide NAD<sup>+</sup> (Sigma-Aldrich, St. Louis, MO, USA), while *LUC* transcribed without NAD<sup>+</sup> was used as a negative control. We then performed NAD capture on these two populations of *LUC* transcripts as previously described (Cahová et al., 2015). Briefly, *LUC* with and without NAD<sup>+</sup> addition was incubated with 4-pentyn-1-ol (Sigma-Aldrich, St. Louis, MO, USA) with or without ADPRC (Sigma-Aldrich, St. Louis, MO, USA) at 37°C for 30 minutes. These reactions were then incubated with Copper-catalyzed azide-alkyne cycloaddition (CuAAC) and biotin azide (Sigma-Aldrich, St. Louis, MO, USA) at 25°C for 30 minutes for to allow the click reaction to occur. Subsequently, Dynabeads MyOne Streptavidin C1 beads (ThermoFisher Scientific, Waltham, MA, USA) were used to pull down the biotinylated RNAs. Different to NAD captureSeq which immediately proceeds to on-bead ligation, reverse transcription of captured RNA, and release of cDNA from streptavidin beads by alkaline digest (Cahová et al., 2015), we added 10 mM EDTA (pH 8.2) and 95% formamide to elute biotinylated RNAs from the streptavidin beads, and eluted RNAs were purified by RNA precipitation with 100% EtOH (NAD-seq). Finally, reverse transcription was performed with gene specific primers (*LUC* specific primer) using SuperScript II (ThermoFisher Scientific, Waltham, MA, USA). Quantitative PCR (qPCR) was performed using SYBR Green 2X master mix (Bimake, Houston, TX, USA) to detect the *LUC* abundance in three biological replicates of each treatment condition using *LUC* specific primers described in Table S8. Significance between differences in detected *LUC* abundance between the various treatments was assessed using a Student's *t* test.

### RNA Extraction

All experiments described in this study were performed with RNA extracted from unopened flower buds, 21-day-old seedlings, or 12-day-old seedlings (as specified) homogenized using a liquid N<sub>2</sub> cooled mortar and pestle. RNA was extracted from homogenate using Qiazol lysis reagent, and further homogenized using QiaShredders (Qiagen, Valencia, CA, USA). RNA was then isolated using Qiagen miRNEasy mini columns (Qiagen, Valencia, CA, USA), as described in the included protocol. All RNA was then treated with RNase-free DNase (Qiagen, Valencia, CA, USA) at room temperature for 30 minutes and subsequently ethanol precipitated.

### *In Vivo* NAD-seq Library Construction

NAD<sup>+</sup> RNA capture was performed by first DNase treating total RNA extracted from two biological replicates of unopened flower buds or 12-day-old seedlings with and with 0.5 μM ABA treatment of Col-0 and *dxo1* mutants as described above for the *LUC* control experiments. The eluted biotinylated RNAs from these NAD<sup>+</sup> RNA capture reactions were precipitated using 100% ethanol, and then fragmented using RNA Fragmentation Reagents (Thermo Fisher Scientific, Waltham, MA, USA). Subsequently, the fragmented RNA samples were treated with T4 polynucleotide kinase (New England Biolabs, Ipswich, MA, USA) to produce RNA fragments with 5' phosphates (5' P) and 3' OHs that are competent for subsequent RNA cloning steps necessary for sequencing library preparation. Sequencing library construction was then performed using the TruSeq Small RNA Sample Prep Kit using the included protocol (Illumina, San Diego, CA, USA) including adaptor ligation, reverse transcription, and PCR amplification with indexed primers as previously described (Zheng et al., 2010; Li et al., 2012; Silverman et al., 2014; Gosai et al., 2015). These sequencing libraries were then treated with Duplex Specific Nuclease (DSN) (Evrogen, Enzo Life Sciences, Farmingdale, NY, USA) to remove highly abundant RNA sequences as previously described (Silverman et al., 2014; Gosai et al., 2015). The resulting libraries were sequenced on an Illumina HiSeq2000 using the standard protocol for 50 base pair single-end sequencing.

### Validation of NAD-seq by NAD-qPCR

Total RNA was extracted from three biological replicates of Col-0 and *dxo1-2* unopened flower buds as described above. Subsequently, 1 nanogram of *in vitro* transcribed *LUC* RNA containing NAD<sup>+</sup> modifications was spiked into 1 μg of total RNAs, and then each sample was divided into two parts evenly. Half was used as the total RNA background, while other half was used to perform NAD<sup>+</sup> RNA capture as described above. Finally, reverse transcription was performed with random hexamers using SuperScript II (Thermo Fisher Scientific, Waltham, MA, USA). Quantification of transcript abundance by qRT-PCR was performed in NAD<sup>+</sup> captured RNAs and total RNAs using SYBR Green 2X master mix (Bimake, Houston, TX, USA) following the manufacturer's protocol with primers listed in Table S8. *LUC* was used as a normalization control for the ΔΔCt analyses. Significance was assessed by Student's *t* test. Three biological replicates were used in these experiments.

### polyA-selected and Total RNA-seq (mRNA- and RNA-seq) Library Construction

For mRNA-seq, two rounds of polyA<sup>+</sup> selection was performed using Dynabeads mRNA DIRECT Purification Kit (Thermo Fisher Scientific, Waltham, MA, USA) on total RNA extracted from unopened flower buds or 12-day-old seedlings with and without 0.5 μM ABA treatment of Col-0 and *dxo1-2* mutants. This polyA<sup>+</sup> RNA was then used as the substrates in RNA-seq library construction as previously described (Anderson et al., 2018). Total RNA-seq library construction was performed similar to mRNA-seq with two exceptions: 1) polyA<sup>+</sup> selection was omitted and 2) the sequencing libraries were subjected to a final DSN treatment (Evrogen, Enzo Life Sciences, Farmingdale, NY, USA) to remove highly abundant RNA sequences as previously described (Silverman et al., 2014; Gosai

et al., 2015). The resulting libraries were sequenced on an Illumina HiSeq2000 using the standard protocol for 50-base pair single-end sequencing.

### smRNA-seq Library Construction

Small RNA sequencing (smRNA-seq) libraries for unopened flower buds from Col-0, *dxo1-2* single mutant, and *rdr6-11 dxo1-2* double mutants were constructed using TruSeq Small RNA Sample Prep Kit using the included protocol (Illumina, San Diego, CA, USA). The resulting libraries were sequenced on an Illumina HiSeq2000 using the standard protocol for 50 base pair single-end sequencing.

### Genome-wide Mapping of Uncapped and Cleaved Transcripts (GMUCT)

GMUCT libraries were constructed and sequenced for all samples described in this study (Col-0 and *dxo1* mutant unopened flower buds and 12-day-old seedlings with and without 0.5  $\mu$ M ABA treatment) as previously described (Willmann et al., 2014). The resulting libraries were sequenced on an Illumina HiSeq2000 using the standard protocol for 50 base pair single-end sequencing.

### Germination Test during ABA Treatment

Seeds of Col-0, *dxo1-1*, *dxo1-2*, and *rdr6-11 dxo1-2* were plated on the  $\frac{1}{2}$  MS (Phytotech Labs, Lenexa, KS, USA) containing 1% sucrose and treated for 48 hours at 4°C. The plates were then transferred to 22°C and grown under long day conditions. To measure seed germination in response to ABA, the  $\frac{1}{2}$  MS (Phytotech Labs, Lenexa, KS, USA) media was supplemented with 0.2  $\mu$ M, 0.5  $\mu$ M, 2  $\mu$ M, or 10  $\mu$ M ABA (Sigma-Aldrich, St. Louis, MO, USA) dissolved in ethanol or ethanol alone that corresponded to the same concentration to act as a control (0  $\mu$ M), and the plates were incubated in a growth chamber horizontally (0.2  $\mu$ M, 0.5  $\mu$ M, and 2  $\mu$ M ABA) or vertically (0 and 10  $\mu$ M). After 7 days, the plates were photographed. These experiments were performed more than 3 times to act as multiple biological replicates. Representative images are shown in Figures 4A and S5A. To assess germination rate, seeds of Col-0, *dxo1-2*, and *rdr6-11 dxo1-2* were sown on  $\frac{1}{2}$  MS without and with 0.5  $\mu$ M ABA and following a 48 hour at 4°C treatment they were grown vertically for 3 days. On day 4, the number of seeds that germinated, as measured by cotyledon emergence, was counted ( $n = 108$  each genotype).

### Liquid Chromatography-High Resolution Mass Spectrometry (LC-HRMS) to Detect Total NAD<sup>+</sup>

15-30 biological replicates of 21-day-old seedlings of Col-0, *dxo1-2*, and *rdr6-11 dxo1-2* were used for detecting free NAD<sup>+</sup>. The seedlings for these genotypes were grown on  $\frac{1}{2}$  MS plates, harvested, and homogenized using a liquid N<sub>2</sub> cooled mortar and pestle. Total NAD<sup>+</sup> was quantified in these powdered tissue samples using quantitative LC-HRMS with stable isotope labeled internal standards as previously described (Frederick et al., 2017).

### qRT-PCR to Detect NAD<sup>+</sup> Biosynthesis Genes

Total RNA extracted from 21-day-old seedlings of Col-0, *dxo1-2*, and *rdr6-11 dxo1-2* as described above was used as the substrate in reverse transcription reactions performed using oligo(dT) primers and SuperScript II (Thermo Fisher Scientific, Waltham, MA, USA). Quantification of transcript abundance (*QPRT*, *NMNAT* and *NADS*) by qRT-PCR was performed using SYBR Green 2X master mix (Bimake, Houston, TX, USA) following the manufacturer's protocol with primers listed in Table S8. *ACT1* (*AT2G37620*) was used as an internal normalization control for the  $\Delta\Delta$ Ct analyses. Significance was assessed by Student's *t* test. Three biological replicates were used in these experiments.

### Transcript Stability Time Course

To measure mRNA stability, we first grew Col-0 and *dxo1-2* mutants seeds vertically on  $\frac{1}{2}$  MS (Phytotech Labs, Lenexa, KS, USA) media without or with 0.5  $\mu$ M ABA (Sigma-Aldrich, St. Louis, MO, USA) as described above. These control and ABA treated seedlings were carefully transferred into  $\frac{1}{2}$  MS (Phytotech Labs, Lenexa, KS, USA) liquid growth media containing 10  $\mu$ M Actinomycin D and 0.6 mM cordycepin (Sigma-Aldrich, St. Louis, MO, USA). Plants were then harvested at 0 and 24 hours post-treatment. Total RNA was extracted as described above and reverse transcribed using oligo dT primers (Thermo Fisher Scientific, Waltham, MA, USA). To measure the stability of NAD<sup>+</sup> capped transcripts as compared to other transcripts from the same genes, total RNAs were performed using NAD<sup>+</sup> capture (see description above), the NAD<sup>+</sup> capped transcripts and other transcripts (supernatants) were purified and reverse transcribed using oligo dT (Thermo Fisher Scientific, Waltham, MA, USA). Quantification of total RNA abundance, NAD<sup>+</sup> capped transcripts abundance and all other transcript populations from the same genes at 0 and 24 hours was performed using qRT-PCR with primers described in Table S8.

## QUANTIFICATION AND STATISTICAL ANALYSIS

### Identification of NAD<sup>+</sup> Capped RNAs

NAD-seq and RNA-seq reads were trimmed to remove the adapter sequences using cutadapt (v1.9.1) with default parameter (Martin, 2011). The trimmed reads were mapped to the Arabidopsis genome (TAIR10) using STAR (version 2.4.2a with "--outFilterMultimapNmax 10 --outFilterMismatchNoverLmax 0.10") (Dobin et al., 2013). Subsequently, read counts for each gene were calculated by htseq-count (HTseq v0.6.0) using the strand-specific parameters (Anders et al., 2015). Finally, negative binomial generalized linear models (DESeq2) (Love et al., 2014) were used to define significantly enriched NAD<sup>+</sup> capped RNAs (false discovery rate < 0.1) in

NAD-seq samples as compared to total RNA-seq samples using the data from two independent biological replicates. All reads were normalized as reads per million (RPM). The NAD<sup>+</sup> capped proportion metric was defined as the log<sub>2</sub> ratio of NAD<sup>+</sup> capped reads of given transcripts as compared to total RNA-seq reads for the corresponding transcript ( $\log_2[\text{RPM}_{\text{NAD-seq}}/\text{RPM}_{\text{RNA-seq}}]$ ). The significant enrichment of gene ontology (GO) terms for the collections of NAD<sup>+</sup> capped RNAs was performed with the gene ontology enrichment analysis using the DAVID tools set at default parameters (Huang et al., 2009).

### Measurement of mRNA Stability Using the Proportion Uncapped Metric

RNA-seq and GMUCT raw reads (50 nt single-end sequences) were trimmed to remove the adapter sequences using cutadapt with default parameters (Martin, 2011). The trimmed reads were aligned to the Arabidopsis genome (TAIR10) using STAR as described above (Dobin et al., 2013). HTSeq was used to calculate the number of raw reads mapping to each given transcript using strand-specific parameters (Anders et al., 2015). The total mapping reads were normalized to reads per million (RPM). Proportion uncapped was defined as the log<sub>2</sub> ratio of normalized GMUCT reads of a given transcript divided by the RNA-seq reads also to each corresponding transcript ( $\log_2[\text{RPM}_{\text{GMUCT}}/\text{RPM}_{\text{RNA-seq}}]$ ) for measuring the general level of RNA degradation as previously described (Anderson et al., 2018).

### Differential Abundance Analysis

Gene counts for each transcript were called using HTseq-count on aligned RNA-seq reads using the parameters “--format=bam --stranded=reverse --mode=intersection-strict”. Differentially abundant transcripts were identified using edgeR (v3.26.6) with the adjusted p-value < 0.05 (Robinson et al., 2010).

### Small RNA Profiling

The smRNA-seq analyses were performed as previously described (Yu et al., 2016). Briefly, all small RNA reads (50 nt single-end sequences) were trimmed to remove the adapter sequences using cutadapt with default parameters (Martin, 2011). The trimmed reads were aligned to all full-length mature mRNAs found in the annotated Arabidopsis genome (TAIR10) using STAR as described above (Dobin et al., 2013). The perfect matching reads mapping to mature mRNAs were extracted and the length distribution of small RNA reads from 20–24 nt were counted in a strand-specific manner. The 21–22 nt small RNAs from both strands of each endogenous mRNA were counted. The edgeR (v3.26.6) (Robinson et al., 2010) analysis package was then used to define mRNAs producing significantly differentially abundant smRNAs between Col-0 and *dxo1* mutant plants with an adjusted p value < 0.05.

### Determination of Library Reproducibility

Read coverage of Arabidopsis transcripts were calculated and normalized using HTseq followed by DESeq2 analysis (Anders et al., 2015; Love et al., 2014) to perform distance measurement and principal component analysis for clustering the samples based on the normalized read counts of Arabidopsis transcripts.

### Construction of a DXO1 Phylogenetic Tree

The protein sequences of DXO1 in 19 representative species including yeast, *C. elegans*, *Drosophila*, mouse, human, and Arabidopsis were downloaded through HomoloGene in NCBI. The multiple alignment of these protein sequences was performed using default parameters of the Molecular Evolutionary Genetics Analysis (MEGA) v5.2 software, and neighbor-joining trees were constructed using MEGA v5.2 (Tamura et al., 2011). The statistical strengths were assessed by bootstraps with 10,000 replicates.

**Developmental Cell, Volume 56**

**Supplemental Information**

**Messenger RNA 5' NAD<sup>+</sup> Capping Is a Dynamic**

**Regulatory Epitranscriptome Mark That Is Required**

**for Proper Response to Abscisic Acid in Arabidopsis**

**Xiang Yu, Matthew R. Willmann, Lee E. Vandivier, Sophie Trefely, Marianne C. Kramer, Jeffrey Shapiro, Rong Guo, Eric Lyons, Nathaniel W. Snyder, and Brian D. Gregory**

**Messenger RNA 5' NAD<sup>+</sup> capping is a dynamic regulatory epitranscriptome mark that is required for proper response to abscisic acid in Arabidopsis**

Xiang Yu, Matthew R. Willmann, Lee E. Vandivier, Sophie Trefely, Marianne C. Kramer, Jeffrey Shapiro, Rong Guo, Eric Lyons, Nathaniel W. Snyder, and Brian D. Gregory

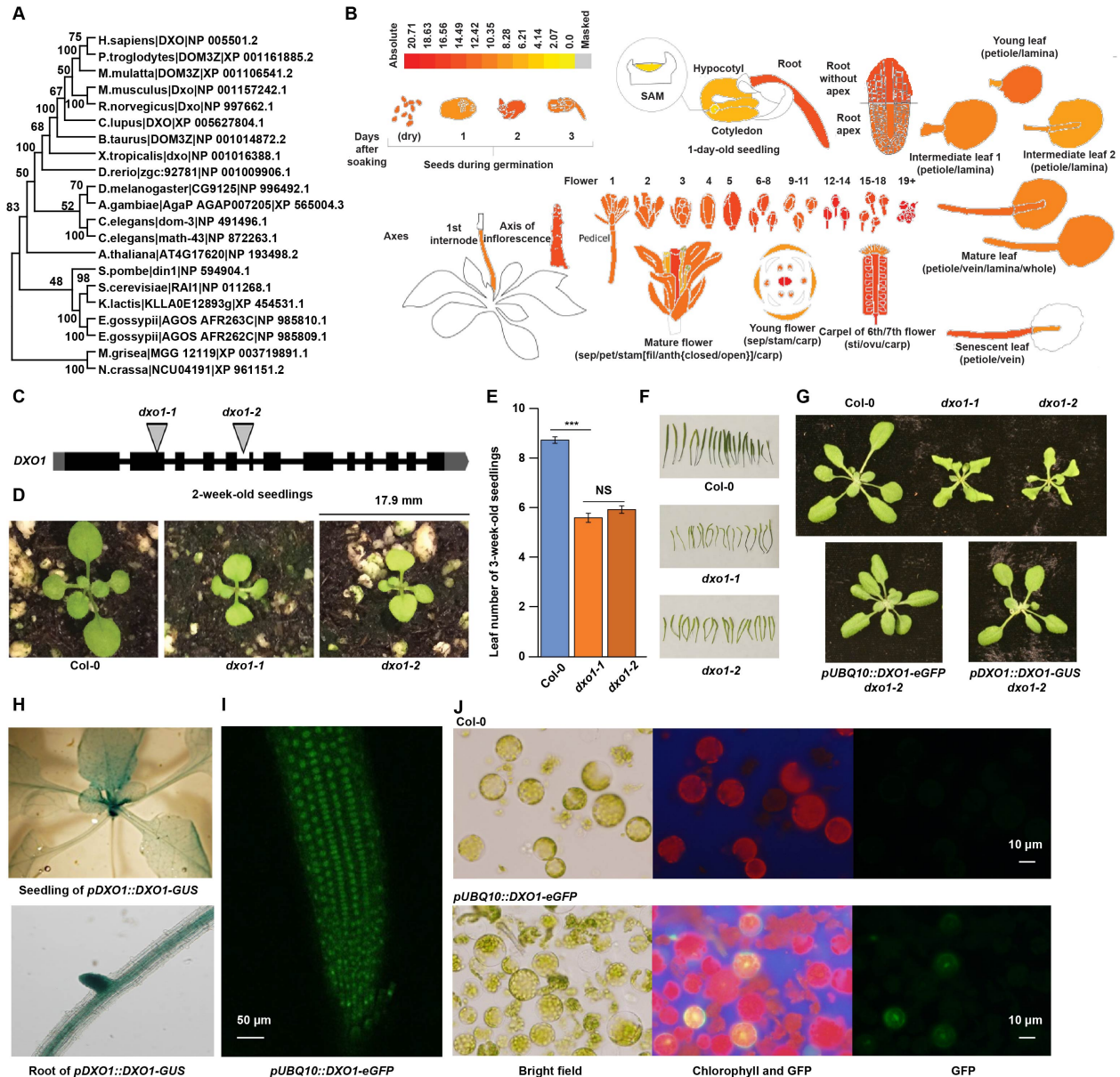


**Figure S1: Growth defects associated with loss of DXO1 function (*dxo1* mutant plants), Related to Figures 1-6.**

(A) A phylogenetic tree of DXO1 proteins from 19 representative species downloaded from NCBI using HomoloGene. (B) A view of the expression pattern of the *DXO1* gene in different Arabidopsis developmental stages and tissues from the Arabidopsis eFP browser (<https://bar.utoronto.ca/efp/cgi-bin/efpWeb.cgi>). Dark red coloration of the specific cartoon tissue representation signifies high levels of *DXO1* RNA are present, whereas bright yellow signifies the opposite. (C) A schematic representation of the *DXO1* gene structure and T-DNA insertion sites. Black boxes represent exons, dark gray boxes represent UTRs, and black lines represent introns. Light gray triangles represent two independent T-DNA insertion sites found in specific SALK T-

DNA insertion lines that correspond to *dxo1-1* (SALK\_103157) and *dxo1-2* (SALK\_032903) mutant alleles. (D) Phenotypes of 2-week-old soil grown Col-0 and *dxo1* mutant plants (*dxo1-1* and *dxo1-2* mutant plants). The *dxo1* mutant plants display a dwarfed phenotype with light green coloration of their leaves as compared to Col-0 plants. Additionally, the leaves and cotyledons of *dxo1* mutants are smaller and develop slower than Col-0 plants. (E) The average leaf number of soil grown 3-week-old Col-0 (N = 12), *dxo1-1* (N = 18), and *dxo1-2* (N = 18) plants. Asterisks denote significant difference in leaf number between Col-0 and *dxo1* mutants at a p-value < 0.001, Student's *t* test. Error bars indicate standard deviation. (F) A picture of siliques from Col-0, *dxo1-1*, and *dxo1-2* mutant plants. The siliques of *dxo1* mutants are lighter green in coloration and smaller in size, denoting less developing seed (reproductive defects) for these mutant plants. (G) Images of soil grown Col-0, *dxo1-1*, *dxo1-2*, *pUBQ10::DXO1-eGFP dxo1-2*, and *pDXO1::DXO1-GUS dxo1-2* plants. It is of note that both the *pDXO1::DXO1-GUS* and *pUBQ10::DXO1-eGFP* transgenic constructs are able to rescue the mutant phenotypes of the *dxo1-2* mutant background demonstrating that these fusion proteins are functional versions of DXO1 that can compensate for the lack of genome-encoded DXO1 in this mutant background. (H) Images of  $\beta$ -Glucuronidase (GUS) stained *pDXO1::DXO1-GUS dxo1-2* soil grown plants (top) and roots from these plants (bottom). (I) Image of GFP signal in the root tip of a *pUBQ10::DXO1-eGFP dxo1-2* soil grown plant. (J) Images of GFP signal in protoplasts isolated from soil grown *pUBQ10::DXO1-eGFP dxo1-2* plants (bottom) and Col-0 (top) as control. Bright field images are on the left, both chlorophyll fluorescence (red signal) and GFP signal can be seen in the middle image, and GFP only signal is visible in the right images. As expected, the Col-0 protoplasts have no GFP signal since this protein is missing in these cells.

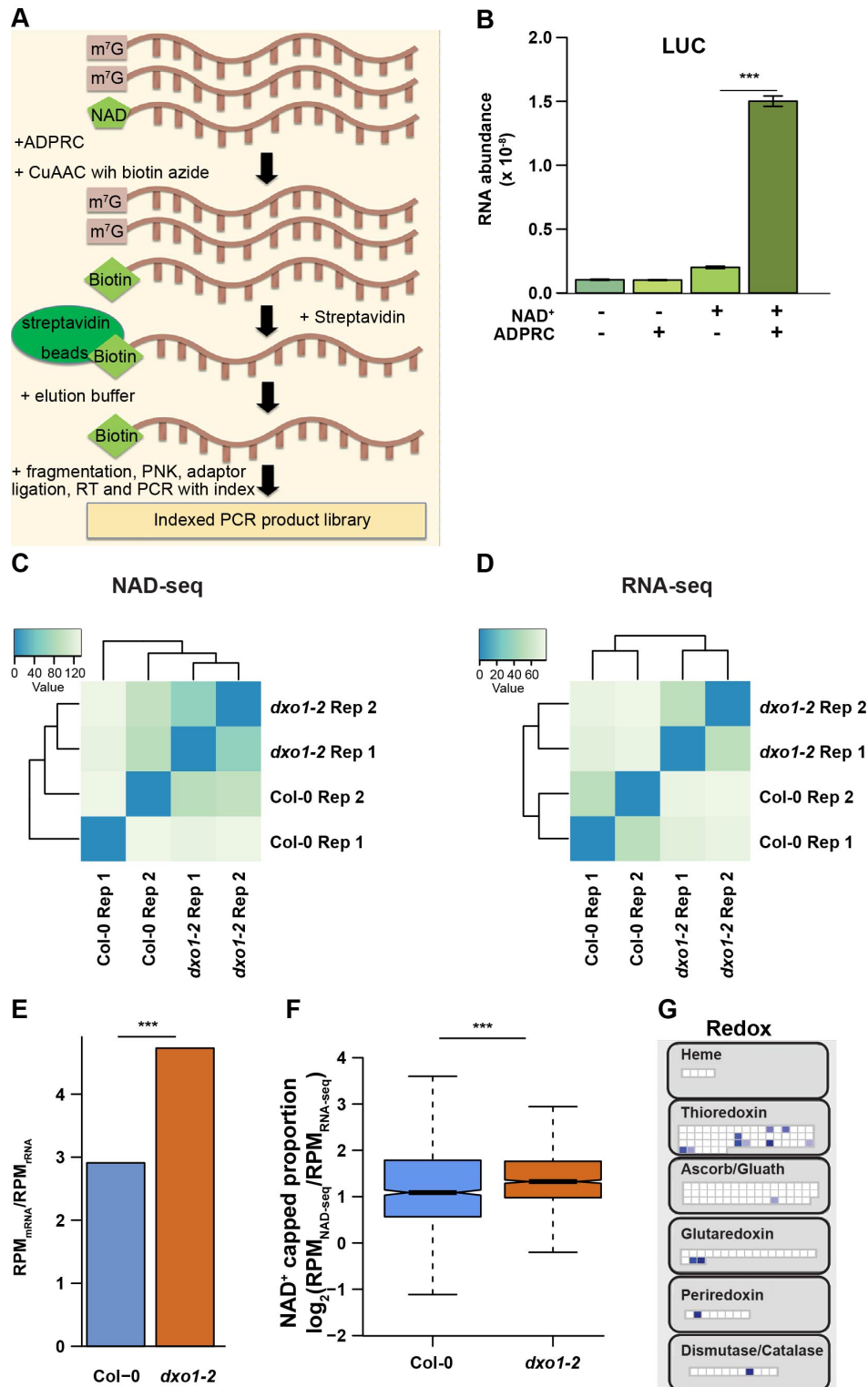


**Figure S2: Development of NAD-CaptureSeq (NAD-seq) for use *in vivo* on two tissues of Col-0 and *dxo1-2* mutant plants, Related to Figures 1-6.**

(A) A schematic diagram showing the processes involved in our NAD-seq approach for use *in vivo* in Arabidopsis plants. (B) RT-qPCR analysis of LUC transcript levels that were *in vitro*

transcribed with and without NAD<sup>+</sup> following the NAD capture that was performed with and without ADPRC treatment. The NAD<sup>+</sup> status of the LUC transcripts and the use of ADPRC are noted in the figure. Error bars indicate  $\pm$  standard error of the mean. \*\*\* denotes p-value < 0.001, Student's *t* test. (C) Clustering analysis of the 2 NAD-seq biological replicates for Col-0 and *dxo1-2* mutant unopened flower buds (4 total libraries). HTSeq was used to count the number of reads mapping to each gene in the TAIR10 transcriptome. Based on these HTSeq read counts from Col-0 and *dxo1-2* NAD-seq replicates, the libraries were clustered based on a correlation analysis via DESeq2 (Love et al., 2014). This analysis revealed high levels of similarity within libraries corresponding to the biological replicates, as each genotype clustered together. (D) Clustering analysis of the 2 RNA-seq biological replicates for Col-0 and *dxo1-2* mutant unopened flower buds (4 total libraries). HTSeq was used to count the number of reads mapping to each gene in the TAIR10 transcriptome. Based on these HTSeq read counts from Col-0 and *dxo1-2* RNA-seq replicates, the libraries were clustered based on a correlation analysis via DESeq2 (Love et al., 2014). This analysis revealed high levels of similarity within libraries corresponding to the biological replicates, as each genotype clustered together. (E) The ratio of reads uniquely mapped to mRNAs as compared to rRNAs ( $\text{RPM}_{\text{mRNA}}/\text{RPM}_{\text{rRNA}}$ ) in NAD-seq libraries of Col-0 and *dxo1-2* mutant unopened flower buds. \*\*\* denotes p-value < 0.001, Mann–Whitney *U* test. (F) The NAD<sup>+</sup> capped proportion ( $\log_2[\text{RPM}_{\text{NAD-seq}}/\text{RPM}_{\text{RNA-seq}}]$ ) for the Col-0 and *dxo1-2* mutant unopened flower bud transcriptomes. \*\*\* denotes p-value < 0.001, Mann-Whitney *U* test. (G) MapMan tool (Thimm et al., 2004) visualization of the NAD<sup>+</sup> capped RNA enrichment in mRNAs encoding proteins involved in redox processes. The color of the blue dot indicates the enriched ratio of NAD<sup>+</sup> capped RNAs in those specific protein-coding mRNAs, with lighter blue indicating less enrichment and darker blue indicating more, while white indicates no enrichment of NAD<sup>+</sup> capping for those mRNAs.

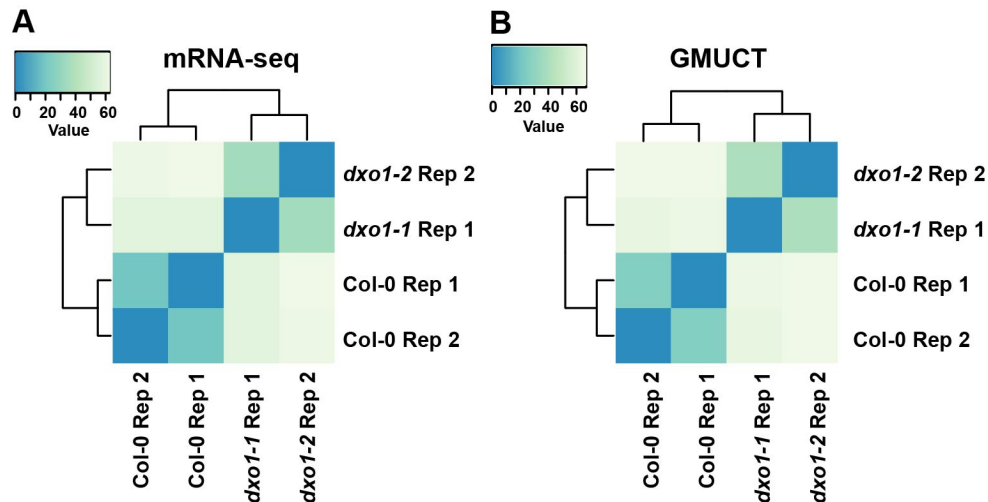


**Figure S3: Reproducibility of mRNA-seq and GMUCT libraries made with RNA from unopened flower buds of Col-0 and *dxo1-2* mutant plants, Related to Figure 2.**

(A) Clustering analysis of the 2 RNA-seq biological replicates for Col-0 and *dxo1-2* mutant unopened flower buds (4 total libraries). HTSeq was used to count the number of reads mapping to each gene in the TAIR10 transcriptome. Based on these HTSeq read counts from Col-0 and *dxo1-2* RNA-seq replicates, the libraries were clustered based on a correlation analysis via DESeq2 (Love et al., 2014). This analysis revealed high levels of similarity within libraries corresponding to the biological replicates, as each genotype clustered together. (B) Clustering analysis of the 2 GMUCT biological replicates for Col-0 and *dxo1-2* mutant unopened flower buds (4 total libraries). HTSeq was used to count the number of reads mapping to each gene in the TAIR10 transcriptome. Based on these HTSeq read counts from Col-0 and *dxo1-2* RNA-seq replicates, the libraries were clustered based on a correlation analysis via DESeq2 (Love et al., 2014). This analysis revealed high levels of similarity within libraries corresponding to the biological replicates, as each genotype clustered together.

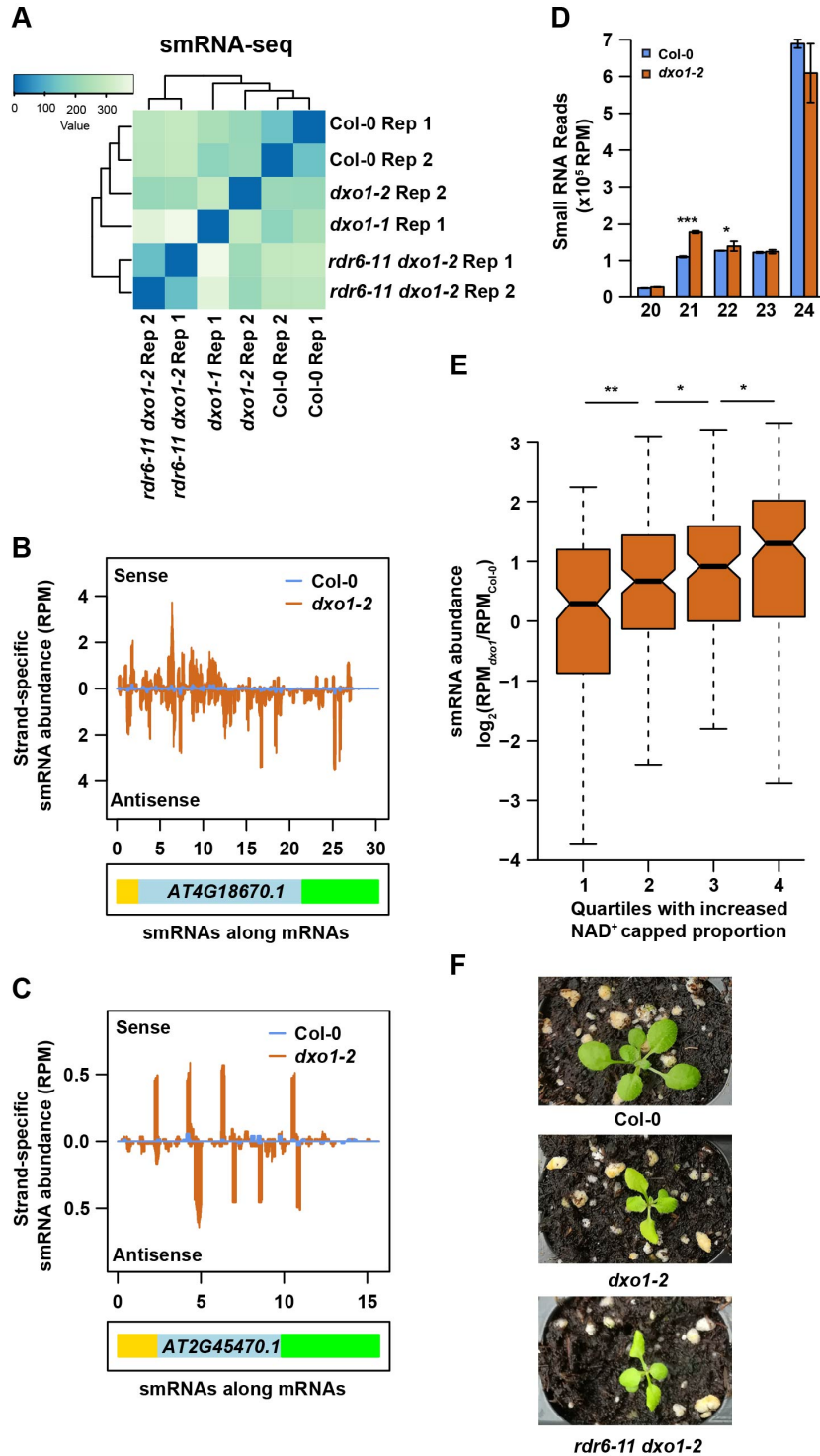


**Figure S4.  $\text{NAD}^+$  capped mRNAs are processed into RDR6-dependent small RNAs in the absence of DXO1 function, but these are not responsible for the phenotypic defects of *dxo1* mutant plants, Related to Figure 3.**

(A) Clustering analysis of the 2 smRNA-seq biological replicates for Col-0, *dxo1* single mutant, and *rdr6 dxo1* double mutant unopened flower buds (6 total libraries). HTSeq was used to count

the number of reads mapping to each gene in the TAIR10 transcriptome. Based on these HTSeq read counts from Col-0, *dxo1* single, and *rdr6 dxo1* double mutant smRNA-seq replicates, the libraries were clustered based on a correlation analysis via DESeq2 (Love et al., 2014). This analysis revealed high levels of similarity within libraries corresponding to the biological replicates, as each genotype clustered together. (B-C) The 21-22 nt smRNA distribution along both (sense and antisense) strands of NAD<sup>+</sup> capped RNAs *AT4G18670* (B) and *AT2G45470* (C) in Col-0 (blue lines) and *dxo1* (orange lines) mutant unopened flower buds. The signal above 0 indicates the reads (RPM) mapped to the forward (sense) strand of each specified mRNA, and the signal below 0 indicates the reads (RPM) mapped to the reverse (anti-sense) strand of each mRNA. The yellow, blue, and green rectangles indicate the 5' UTR, CDS, and the 3' UTR of each mRNA, respectively. (D) The length distribution of small RNAs from protein-coding RNAs in Col-0 and *dxo1* mutant unopened flower buds. \* and \*\*\* denote p-value < 0.05 and 0.001, respectively, Mann–Whitney *U* test. Error bars indicate the mean  $\pm$  1 standard error. (E) The change in small RNA abundance ( $\log_2[\text{RPM}_{dxo1}/\text{RPM}_{Col-0}]$ ) for four quartiles of NAD<sup>+</sup> capped transcripts based on increasing levels of NAD<sup>+</sup> capped proportion ( $\log_2[\text{RPM}_{NAD-seq}/\text{RPM}_{RNA-seq}]$ ) values, with quartile 1 having the lowest values and 4 having the highest. \* and \*\* denote p-value < 0.05 and 0.01, respectively, Mann–Whitney *U* test. (F) The phenotypes of 2-week-old Col-0, *dxo1-2* single, and *rdr6-11 dxo1-2* double mutant plants. The *dxo1-2* single and *rdr6-11 dxo1-2* double mutant plants have nearly indistinguishable phenotypes from one another indicating that the smRNAs produced from NAD<sup>+</sup> capped mRNAs in the absence of DXO1 function are not responsible for the mutant phenotypes of *dxo1* mutant plants.

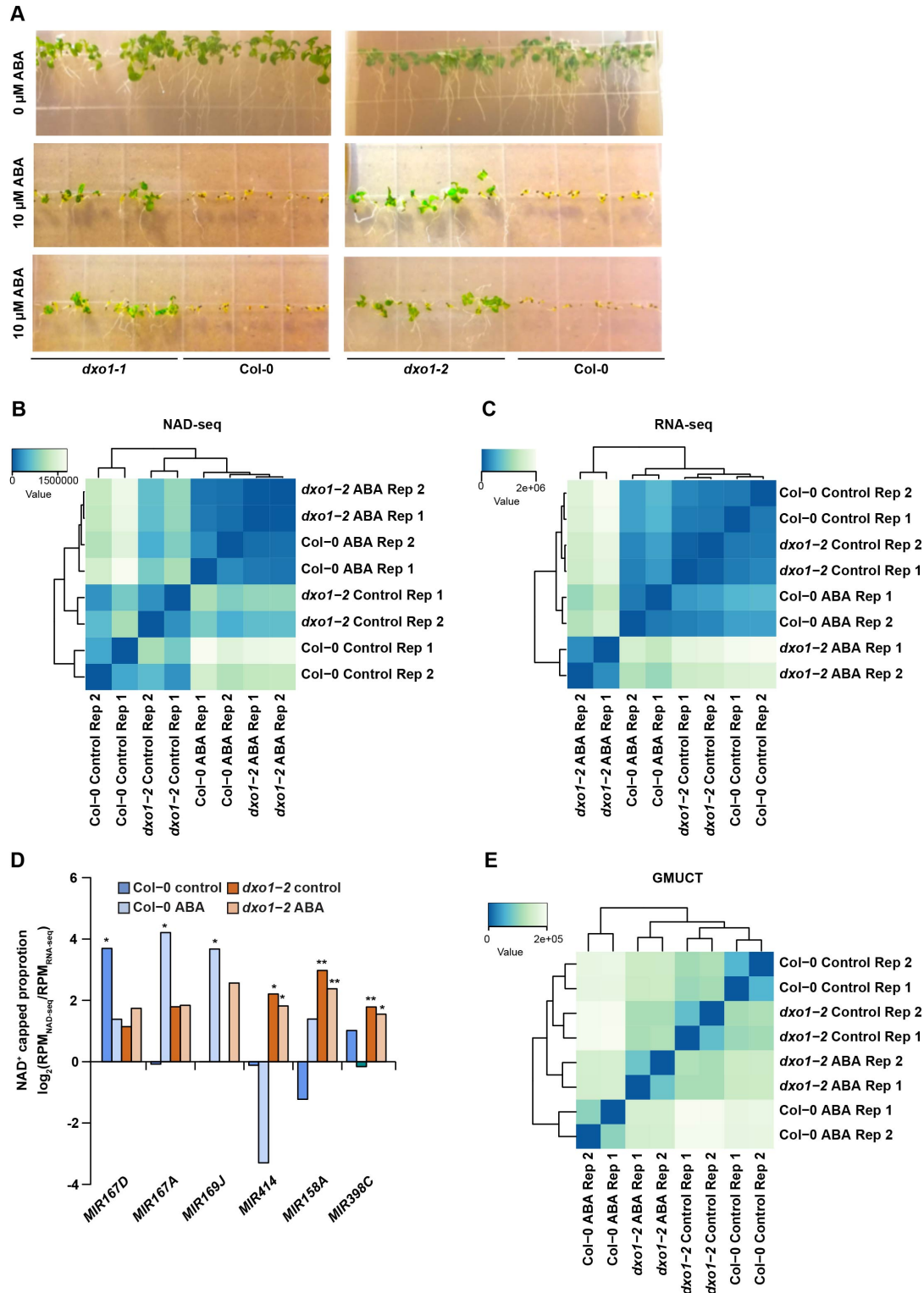


**Figure S5: DXO1 is required for proper ABA response and this plant hormone remodels the NAD<sup>+</sup> capped transcriptome, Related to Figures 4-6.**

(A) Representative images of seed germination of 7-day-old Col-0, *dxo1-1*, and *dxo1-2* seedlings grown on the 1/2 MS plates with 0 and 10  $\mu$ M ABA. (B) Clustering analysis of the 2 NAD-seq

biological replicates for 12-day old Col-0 and *dxo1-2* seedlings without and with 0.5  $\mu$ M ABA treatment (8 total libraries). HTSeq was used to count the number of reads mapping to each gene in the TAIR10 transcriptome. Based on these HTSeq read counts from Col-0 and *dxo1-2* NAD-seq replicates, the libraries were clustered based on a correlation analysis via DESeq2 (Love et al., 2014). This analysis revealed high levels of similarity within libraries corresponding to the biological replicates, as each genotype and treatment clustered together. (C) Clustering analysis of the 2 RNA-seq biological replicates for 12-day old Col-0 and *dxo1-2* seedlings without and with 0.5  $\mu$ M ABA treatment (8 total libraries). HTSeq was used to count the number of reads mapping to each gene in the TAIR10 transcriptome. Based on these HTSeq read counts from Col-0 and *dxo1-2* RNA-seq replicates, the libraries were clustered based on a correlation analysis via DESeq2 (Love et al., 2014). This analysis revealed high levels of similarity within libraries corresponding to the biological replicates, as each genotype and treatment clustered together. (D) The NAD<sup>+</sup> capped proportion ( $\log_2[\text{RPM}_{\text{NAD-seq}}/\text{RPM}_{\text{RNA-seq}}]$ ) of identified NAD<sup>+</sup> capped primary microRNA transcripts in 12-day-old Col-0 or *dxo1-2* mutant seedlings without and with 0.5  $\mu$ M ABA treatment. \* and \*\* denote significant adjusted p-value < 0.05 and 0.01, negative binomial generalized linear models. (E) Clustering analysis of the 2 GMUCT biological replicates for 12-day-old Col-0 and *dxo1-2* mutant seedlings without and with 0.5  $\mu$ M ABA treatment (8 total libraries). HTSeq was used to count the number of reads mapping to each gene in the TAIR10 transcriptome. Based on these HTSeq read counts from Col-0 and *dxo1-2* GMUCT replicates, the libraries were clustered based on a correlation analysis via DESeq2 (Love et al., 2014). This analysis revealed high levels of similarity within libraries corresponding to the biological replicates, as each genotype and treatment clustered together.

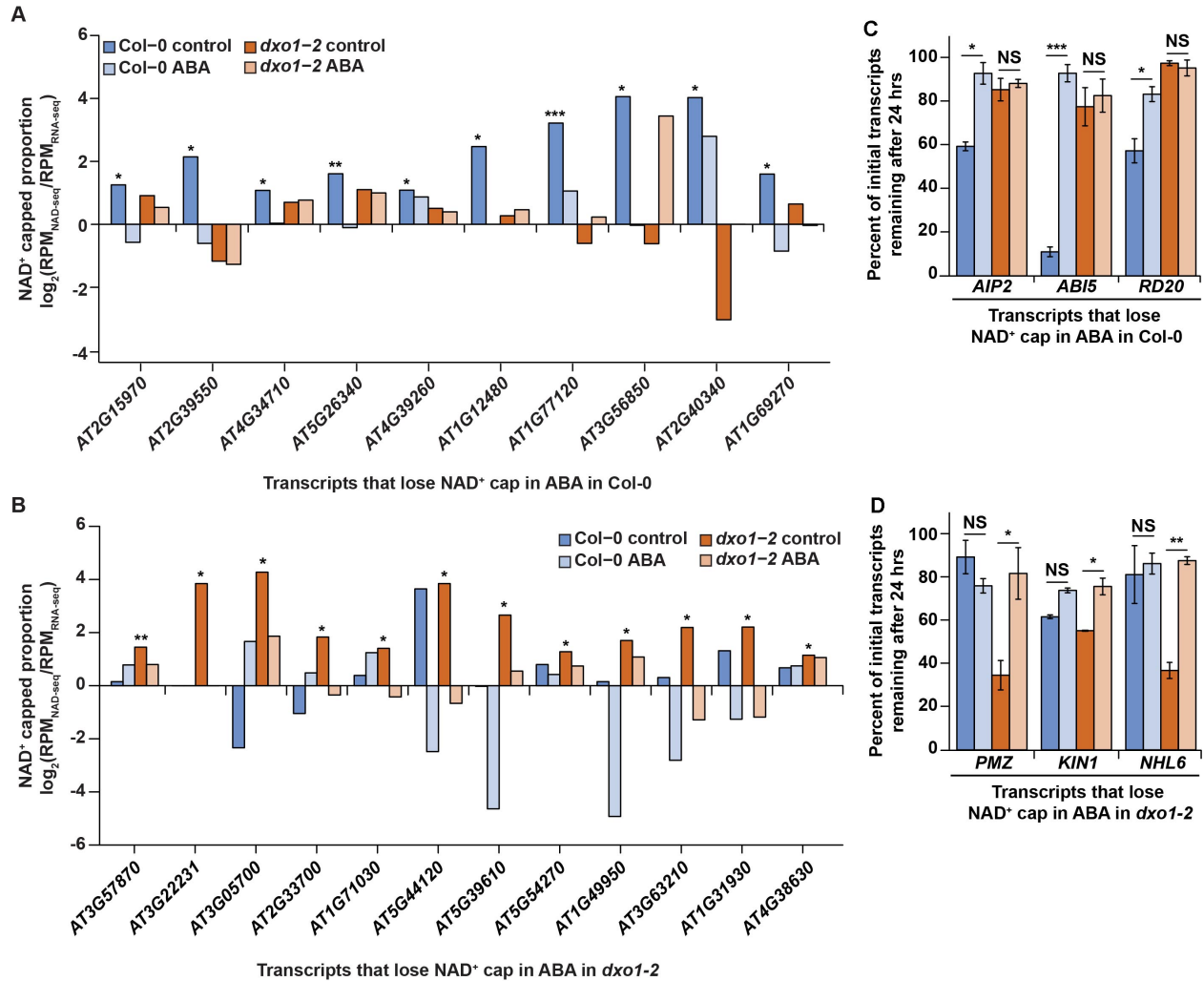


**Figure S6: Transcripts encoding master regulators of ABA response demonstrate dynamic 5' end NAD<sup>+</sup> capping upon ABA treatment, Related to Figure 6.**

(A) NAD<sup>+</sup> capped proportion ( $\log_2[\text{RPM}_{\text{NAD-seq}}/\text{RPM}_{\text{RNA-seq}}]$ ) in Col-0 (blue bars) and *dxo1-2* (orange bars) in the absence (darker colors) or presence (lighter colors) of 0.5  $\mu\text{M}$  ABA for ABA-responsive mRNAs that specifically contain a NAD<sup>+</sup> cap in Col-0. Ten additional examples of the total of 13 mRNAs in this group are shown. (B) NAD<sup>+</sup> capped proportion ( $\log_2[\text{RPM}_{\text{NAD-seq}}/\text{RPM}_{\text{RNA-seq}}]$ ) in Col-0 (blue bars) and *dxo1-2* (orange bars) in the absence (darker colors) or presence (lighter colors) of 0.5  $\mu\text{M}$  ABA for ABA-responsive mRNAs that specifically contain a NAD<sup>+</sup> cap in *dxo1-2*. Twelve additional examples of the total of 15 mRNAs in this group are shown. (A-B) \*, \*\*, and \*\*\* denote p-value < 0.05, 0.01, and 0.001, respectively, negative binomial generalized linear model. (C-D) Percent of *ABI5*, *AIP2*, and *RD20* (C) (three of the ABA-responsive mRNAs that specifically contain a NAD<sup>+</sup> cap in Col-0 without ABA treatment but not after) or *PMZ*, *KIN1*, and *NHL6* (D) (three of the ABA-responsive mRNAs that

specifically contain a NAD<sup>+</sup> cap in *dxo1-2* without ABA treatment but not after) transcripts remaining 24 hours post treatment with transcription inhibitors in 12-day-old seedlings without and with 0.5 μM ABA treatment of Col-0 (blue and light blue bars, respectively) and *dxo1-2* mutants (orange and light orange bars, respectively). The indicated genes producing NAD<sup>+</sup> capped transcripts were chosen from our proportion uncapped data (Figures 5D-E) and assayed. \*, \*\*, and \*\*\* denotes p-value < 0.05, 0.01, and 0.001, Student's *t* test, two-tailed.